Supporting Information for

Discovery of a monomeric green fluorescent protein sensor for chloride by structure-guided bioinformatics

Weicheng Peng[†,‡], Caden C. Maydew[†], Hiu Kam[†], Jacob K. Lynd[†], Jasmine N. Tutol[†], Shelby M. Phelps[†], Sameera Abeyrathna[†], Gabriele Meloni[†], and Sheel C. Dodani[†]*

[†]Departments of Chemistry and Biochemistry and [‡]Biological Sciences, The University of Texas at Dallas, Richardson, Texas 75080

*sheel.dodani@utdallas.edu

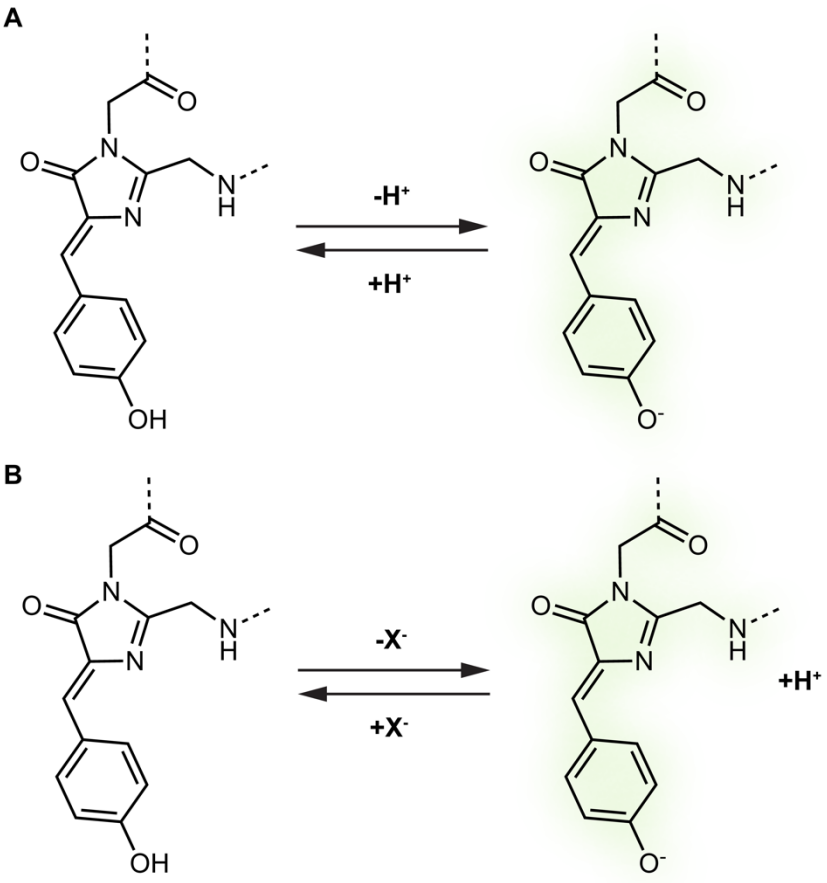

Figure S1. (A) pH- and (B) anion-dependent chromophore equilibrium for avYFP-H148Q.

avYFP-H148Q	100.00	51.29	83.19
phiYFP	51.29	100.00	51.29
GFPxm163	83.19	51.29	100.00

Figure S2. Percent identity matrix of avYFP-H148Q (PDB ID: 1F09), phiYFP (UniProt ID: Q6RYS7), and GFPxm163 (UniProt ID: Q8WTC8).

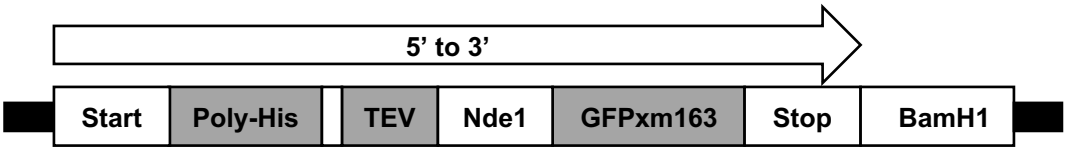

GGATCCATGGGCAGCAGCCATCATCATCATCATCACAGCAGCGGCGAGAATCTTTATTTTCAGGGCCATA
TGAGCAAGGGCGAGGAACTGTTCACCGGCATCGTGCCGGTTCTGATTGAGCTGGACGGTGATGTGCACGG
CCACAAATTTAGCGTTCGTGGCGAGGGTGAAGGTGATGCGGATTACGGCAAGCTGGAAATCAAATTCATT
TGCACCACCGGTAAACTGCCGGTTCCGTGGCCGACCCTGGTTACCACCCTGGGTTACGGCATCCAGTGCT
TTGCGCGTTATCCGGAGCACATGAAGATGAACGACTTCTTTAAAAGCGCGATGCCGGAGGGTTACATCCA
GGAACGTACCATTTTCTTTCAAGACGATGGCAAGTACAAGACCCGTGGCGAGGTGAAATTCGAAGGTGAT
ACCCTGGTTAACCGTATCGAGCTGAAGGGCATGGACTTCAAAGAAGATGGTAACATTCTGGGCCACAAGC
TGGAGTACAACTTTAACAGCCACAACGTGTATATCATGCCGGACAAAGCGAACAACGGTCTGAAGGTTAA
CTTTAAAATCCGTCACAACATTGAAGGTGGCGGTGTGCAGCTGGCGGACCACTACCAAACCAACGTGCCG
CTGGGTGATGGCCCGGTTCTGATCCCGATTAACCACTACCTGAGCTATCAAACCGCGATTAGCAAGGACC
GTAACGAGACCCGTGATCACATGGTTTTCCTGGAATTCTTTAGCGCGTGCGGTCACACCCACGGCATGGA
TGAACTGTATAAATAAGGATCC

MGSSHHHHHHSSGENLYFQGHMSKGEELFTGIVPVLIELDGDVHGHKFSVRGEGEGDADYGKLEIKFICT
TGKLPVPWPTLVTTLGYGIQCFARYPEHMKMNDFFKSAMPEGYIQERTIFFQDDGKYKTRGEVKFEGDTL
VNRIELKGMDFKEDGNILGHKLEYNFNSHNVYIMPDKANNGLKVNFKIRHNIEGGGVQLADHYQTNVPLG
DGPVLIPINHYLSYQTAISKDRNETRDHMVFLEFFSACGHTHGMDELYK

Figure S3. Schematic of the GFPxm163-pET-28a(+)-TEV plasmid design for protein expression in *Escherichia coli* with the nucleotide (top) and amino acid (bottom) sequences used in this study.

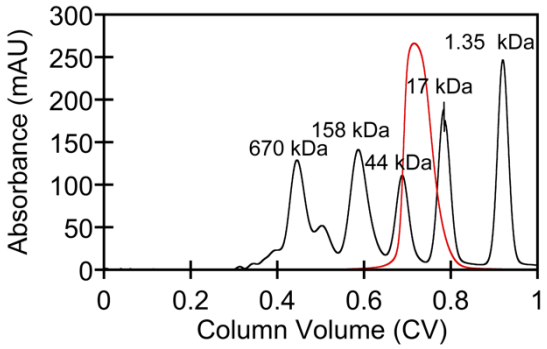

Figure S4. Representative size-exclusion chromatography chromatogram of GFPxm163 in 200 mM phosphate buffer at pH 7.5. The elution peak of GFPxm163 (absorbance at 512 nm) is shown in red, and the elution peaks of the protein standard (absorbance at 280 nm) are shown in black. From left to right, the protein standards are thyroglobulin, γ-globulin, ovalbumin, myoglobin, and vitamin B12.

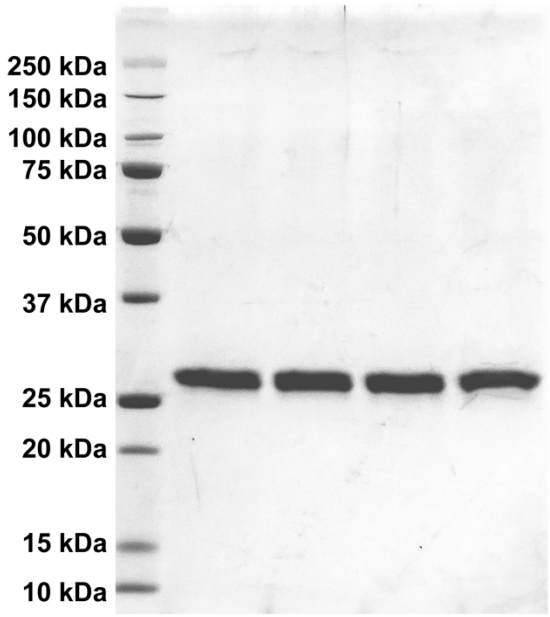

Figure S5. Representative Coomassie-stained SDS-PAGE gel of all GFPxm163 protein preparations used in this study. The expected molecular weight of GFPxm163 is ~29 kDa.

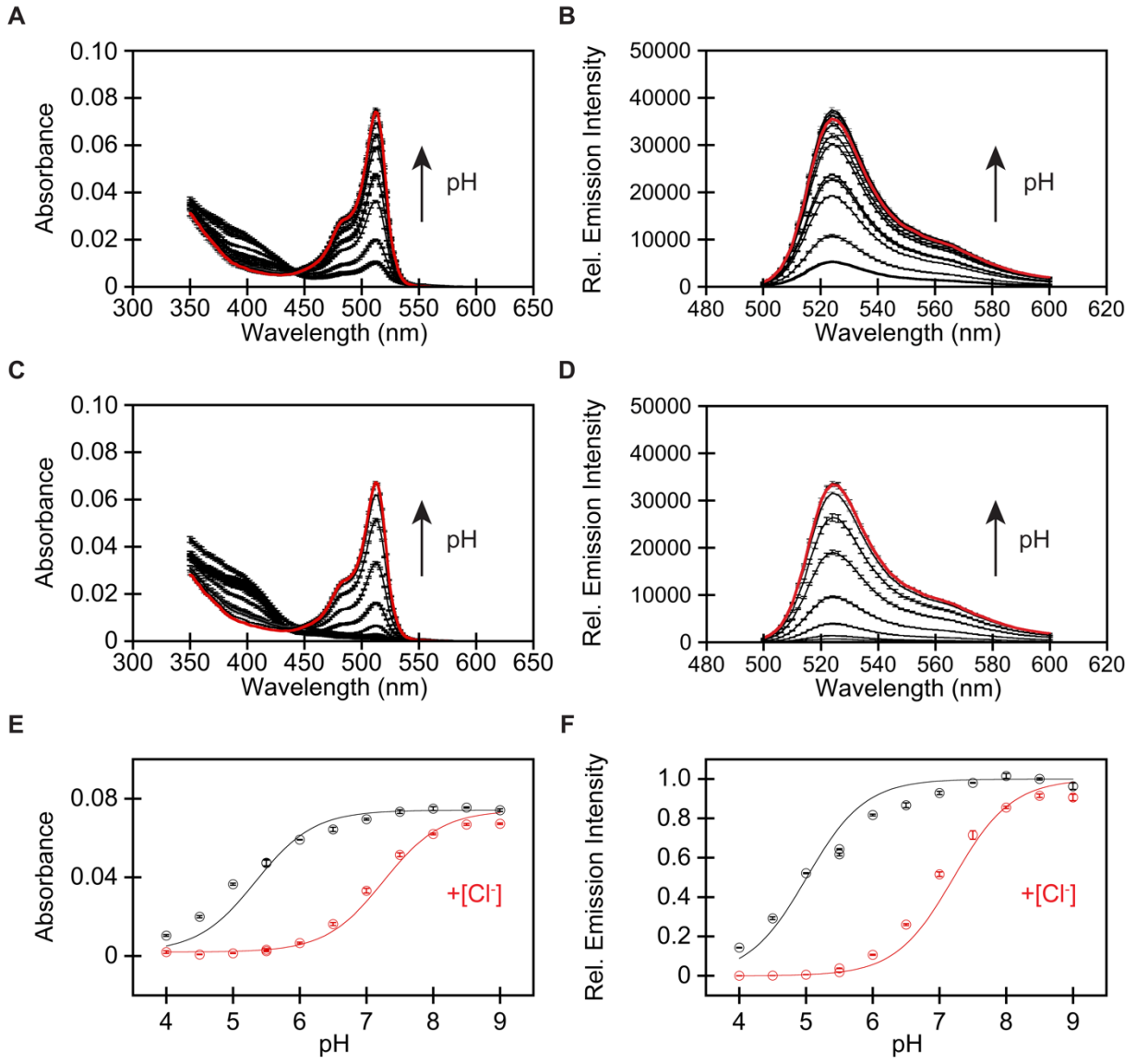

Figure S6. (A) Absorbance and (B) emission spectra of GFPxm163 from pH 4 (bold black) to pH 9 (red). (C) Absorbance and (D) emission spectra of GFPxm163 from pH 4 (bold black) to pH 9 (red) in the presence of 512 mM Cl^-. (E) Absorbance-dependent pK_a curve of GFPxm163 with 0 mM (black) and 512 mM (red) Cl^-. The pK_a values in the absence and presence of chloride are 5.15 ± 0.06 and 7.13 ± 0.04, respectively. (F) Emission-dependent pK_a curve of GFPxm163 with 0 mM (black) and 512 mM (red) Cl^-. The pK_a values in the absence and presence of chloride are 5.23 ± 0.04 and 7.04 ± 0.01, respectively. Data is shown for one of two protein preparations each measured in triplicate and reported as an average with the standard error of the mean (S.E.M.). Data for the second protein preparation is shown in Figure S7. All experiments were carried out at room temperature (24–26 °C) with 1.2 μM of protein in 50 mM sodium acetate buffer for pH 4–5.5 or 50 mM sodium phosphate buffer for pH 5.5–9. Absorbance was collected from 350–600 nm. Excitation was provided at 480 nm, and emission was collected from 500–600 nm.

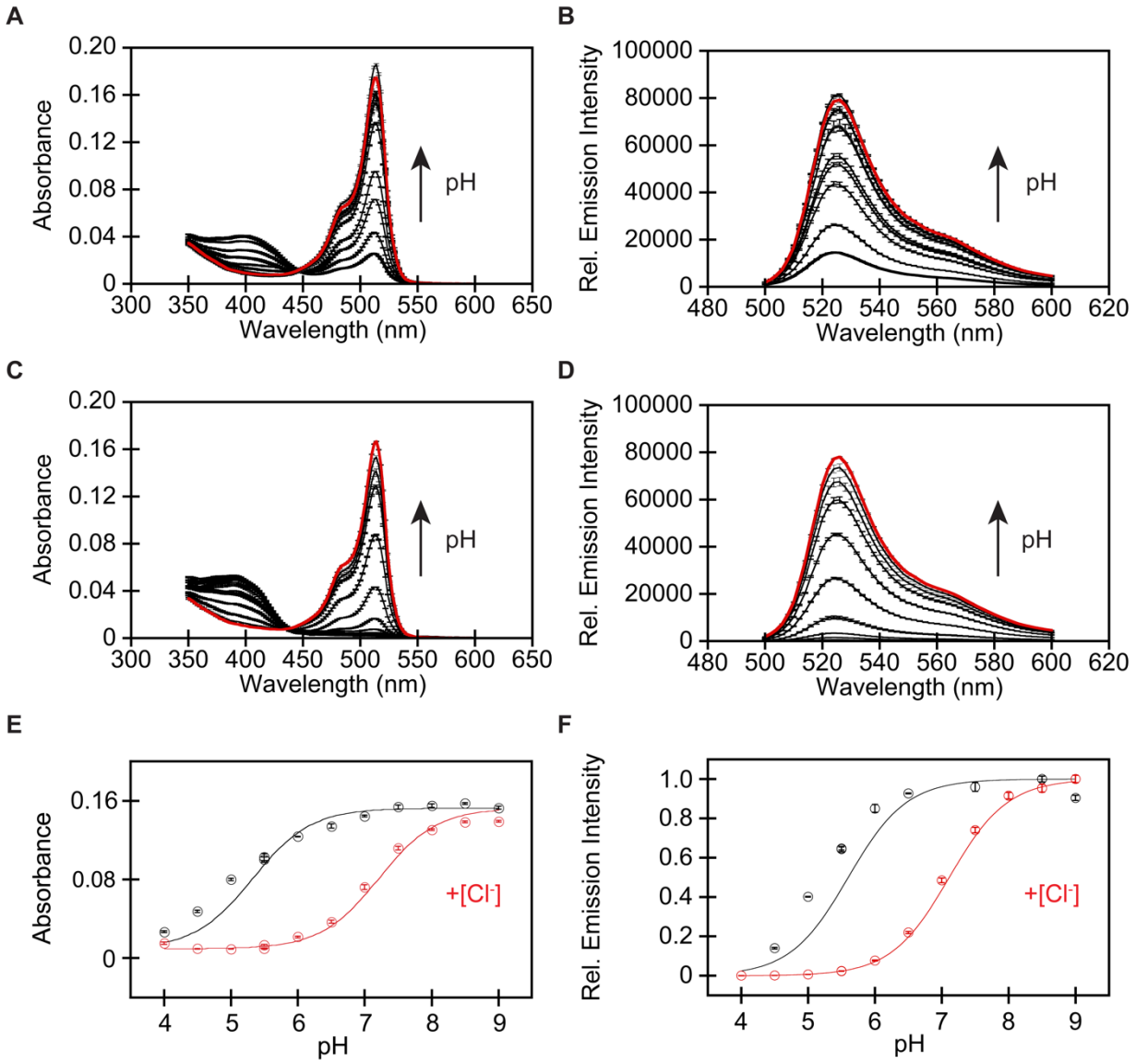

Figure S7. (A) Absorbance and (B) emission spectra of GFPxm163 from pH 4 (bold black) to pH 9 (red). (C) Absorbance and (D) emission spectra of GFPxm163 from pH 4 (bold black) to pH 9 (red) in the presence of 512 mM Cl^-. (E) Absorbance-dependent pK_a curve of GFPxm163 with 0 mM (black) and 512 mM (red) Cl^-. The pK_a values in the absence and presence of chloride are 5.42 ± 0.08 and 6.98 ± 0.04, respectively. (F) Emission-dependent pK_a curve of GFPxm163 with 0 mM (black) and 512 mM (red) Cl^-. The pK_a values in the absence and presence of chloride are 5.12 ± 0.07 and 7.02 ± 0.04, respectively. Data is shown for one of two protein preparations each measured in triplicate and reported as an average with the S.E.M. Data for the first protein preparation is shown in Figure S6. All experiments were carried out at room temperature (24–26 °C) with 2.3 μM of protein in 50 mM sodium acetate buffer for pH 4–5.5 or 50 mM sodium phosphate buffer for pH 5.5–9. Absorbance was collected from 350–600 nm. Excitation was provided at 480 nm, and emission was collected from 500–600 nm.

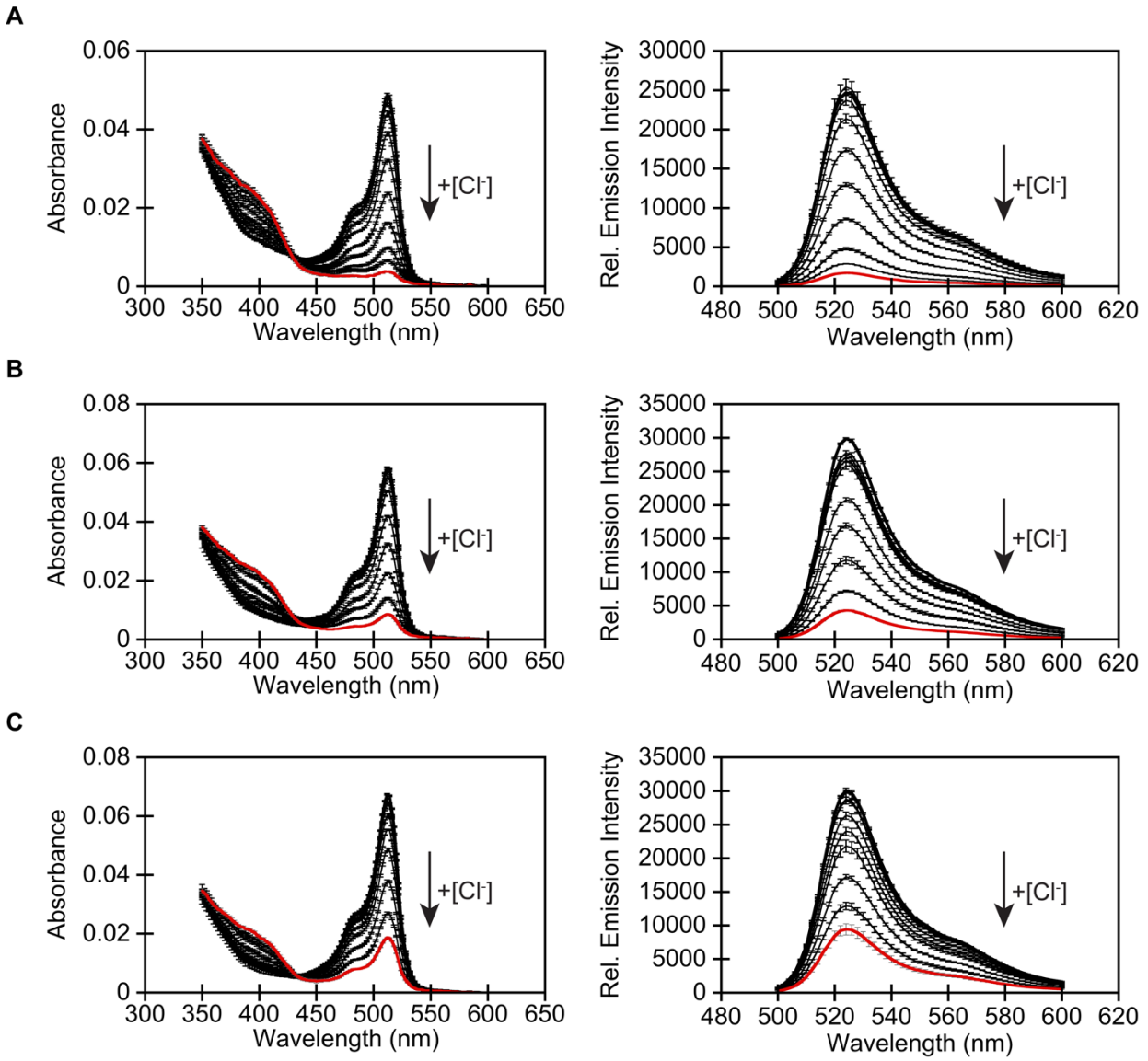

Figure S8. Absorbance (left) and emission spectra (right) of GFPxm163 at (A) pH 6, (B) pH 6.5, and (C) pH 7 in the presence of 0 (bold black), 2, 4, 8, 16, 32, 64, 128, 256, and 512 (red) mM Cl^-. Data is shown for one of two protein preparations each measured in triplicate and reported as an average with the S.E.M. Data for the second protein preparation is shown in Figure S9. All experiments were carried out at room temperature (24–26 °C) with 1 μM of protein in the 50 mM sodium phosphate buffer for pH 6–7. Absorbance was collected from 350–600 nm. Excitation was provided at 480 nm, and emission was collected from 500–600 nm.

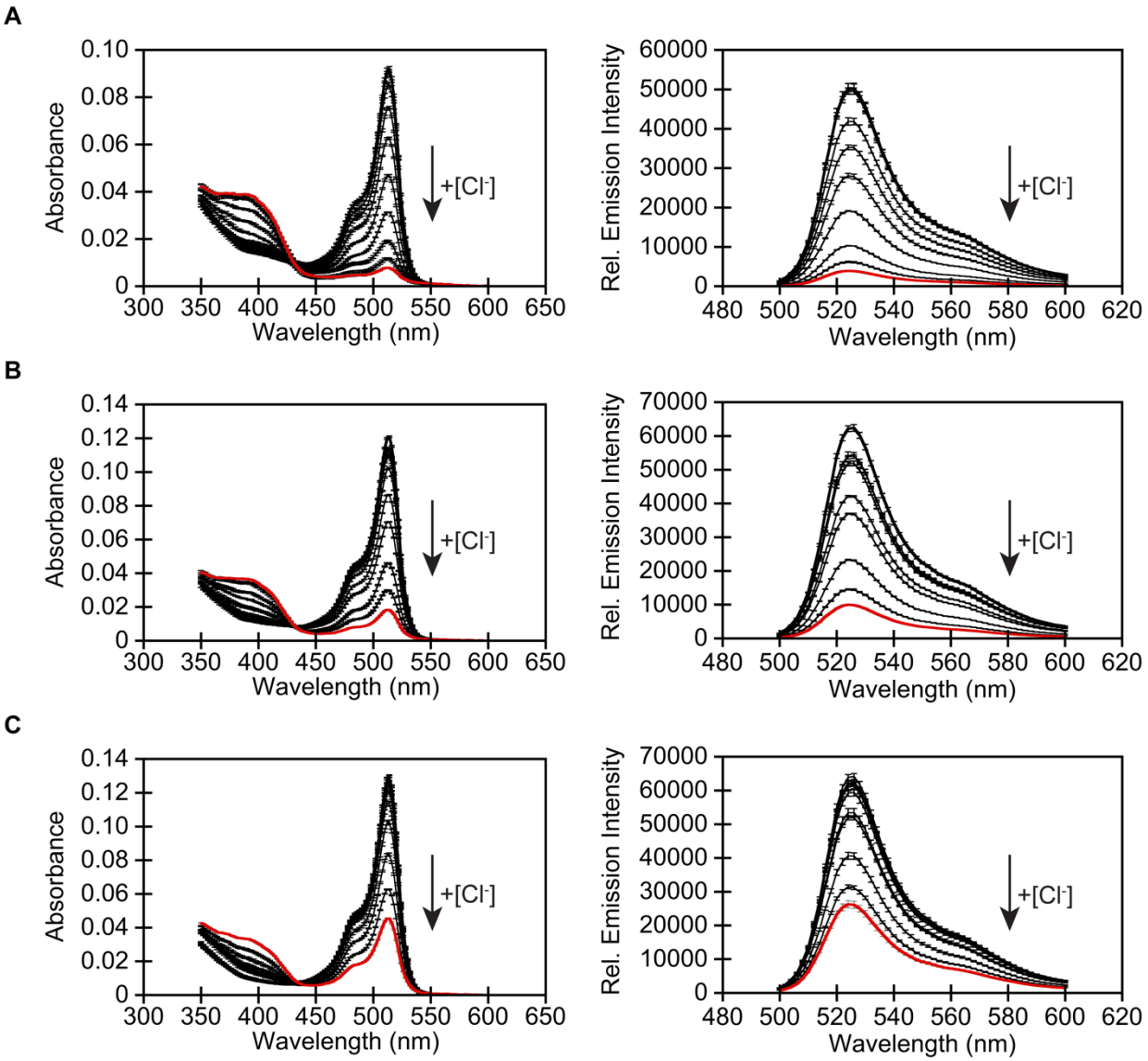

Figure S9. Absorbance (left) and emission spectra (right) of GFPxm163 at (A) pH 6, (B) pH 6.5, and (C) pH 7 in the presence of 0 (bold black), 2, 4, 8, 16, 32, 64, 128, 256, and 512 (red) mM Cl^-. Data is shown for one of two protein preparations each measured in triplicate and reported as an average with the S.E.M. Data for the first protein preparation is shown in Figure S8. All experiments were carried out at room temperature (24–26 °C) with 1.7 μM of protein in the 50 mM sodium phosphate buffer for pH 6–7. Absorbance was collected from 350–600 nm. Excitation was provided at 480 nm, and emission was collected from 500–600 nm.

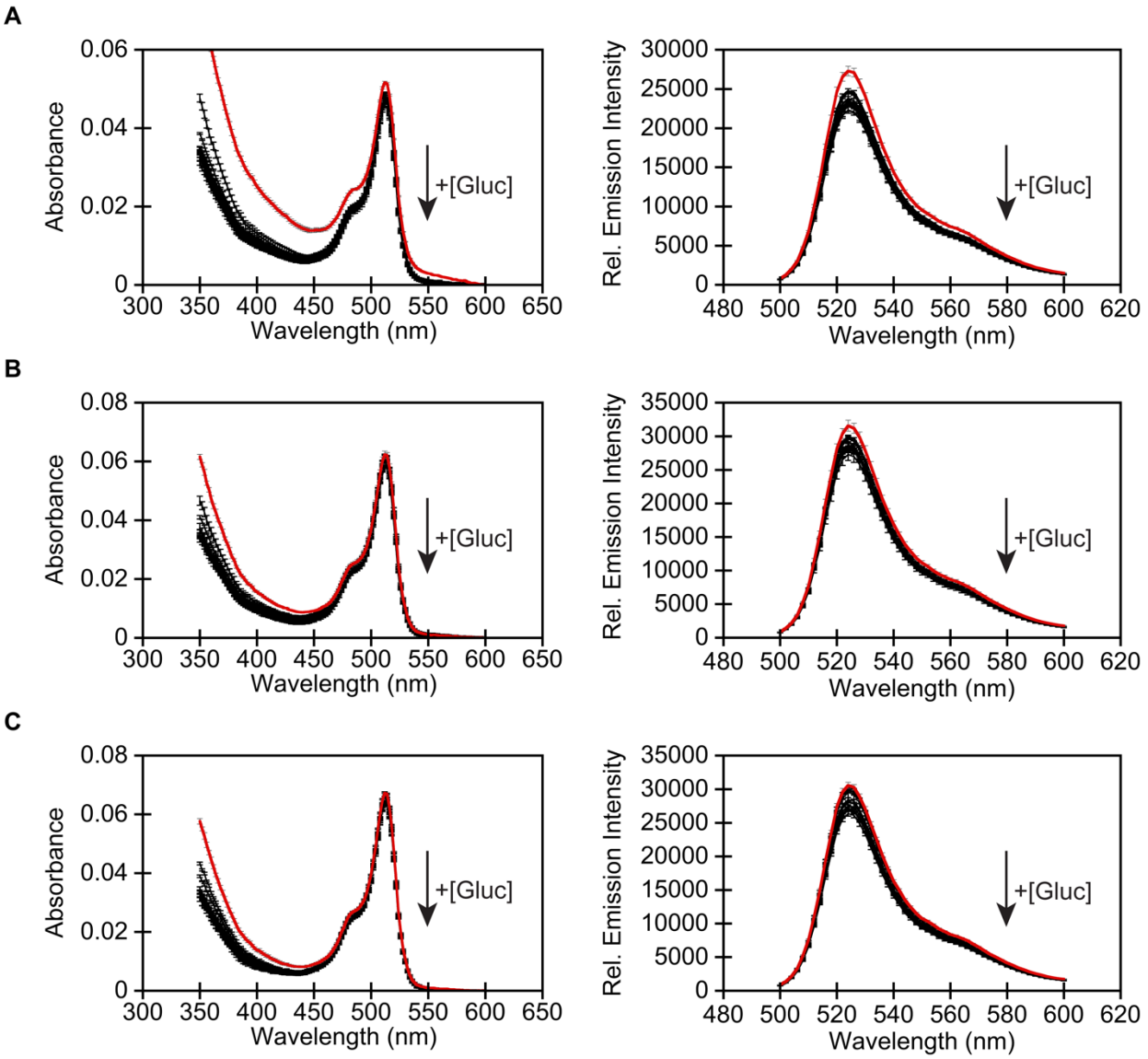

Figure S10. Absorbance (left) and emission spectra (right) of GFPxm163 at (A) pH 6, (B) pH 6.5, and (C) pH 7 in the presence of 0 (bold black), 2, 4, 8, 16, 32, 64, 128, 256, and 512 (red) mM Gluc. Data is shown for one of two protein preparations each measured in triplicate and reported as an average with the S.E.M. Data for the second protein preparation is shown in Figure S11. All experiments were carried out at room temperature (24–26 °C) with 1 μM of protein in the 50 mM sodium phosphate buffer for pH 6–7. Absorbance was collected from 350–600 nm. Excitation was provided at 480 nm, and emission was collected from 500–600 nm. Abbreviation: Gluconate, Gluc.

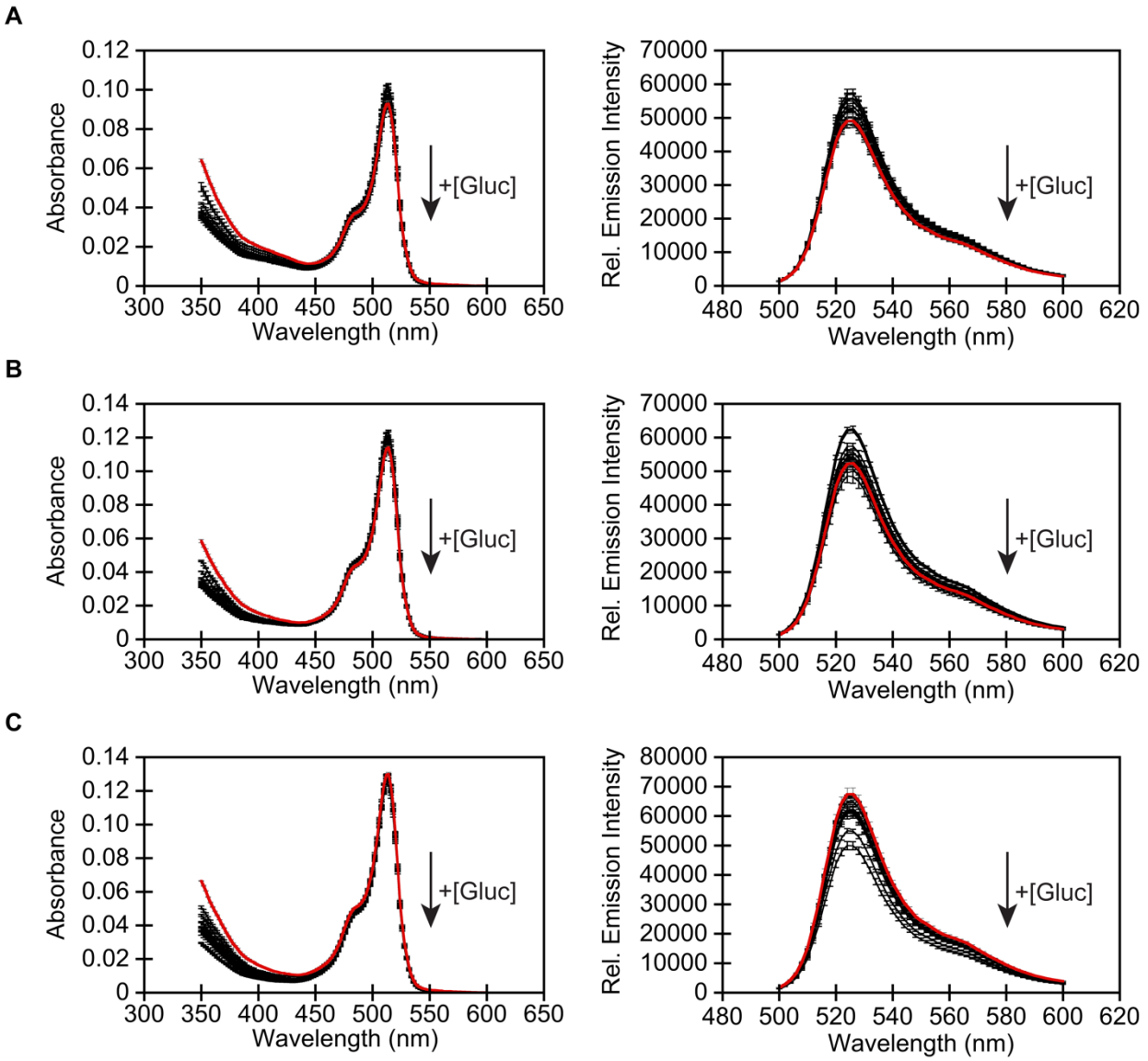

Figure S11. Absorbance (left) and emission spectra (right) of GFPxm163 at (A) pH 6, (B) pH 6.5, and (C) pH 7 in the presence of 0 (bold black), 2, 4, 8, 16, 32, 64, 128, 256, and 512 (red) mM Gluc. Data is shown for one of two protein preparations each measured in triplicate and reported as an average with the S.E.M. Data for the first protein preparation is shown in Figure S10. All experiments were carried out at room temperature (24–26 °C) with 1.7 μM of protein in the 50 mM sodium phosphate buffer for pH 6–7. Absorbance was collected from 350–600 nm. Excitation was provided at 480 nm, and emission was collected from 500–600 nm.

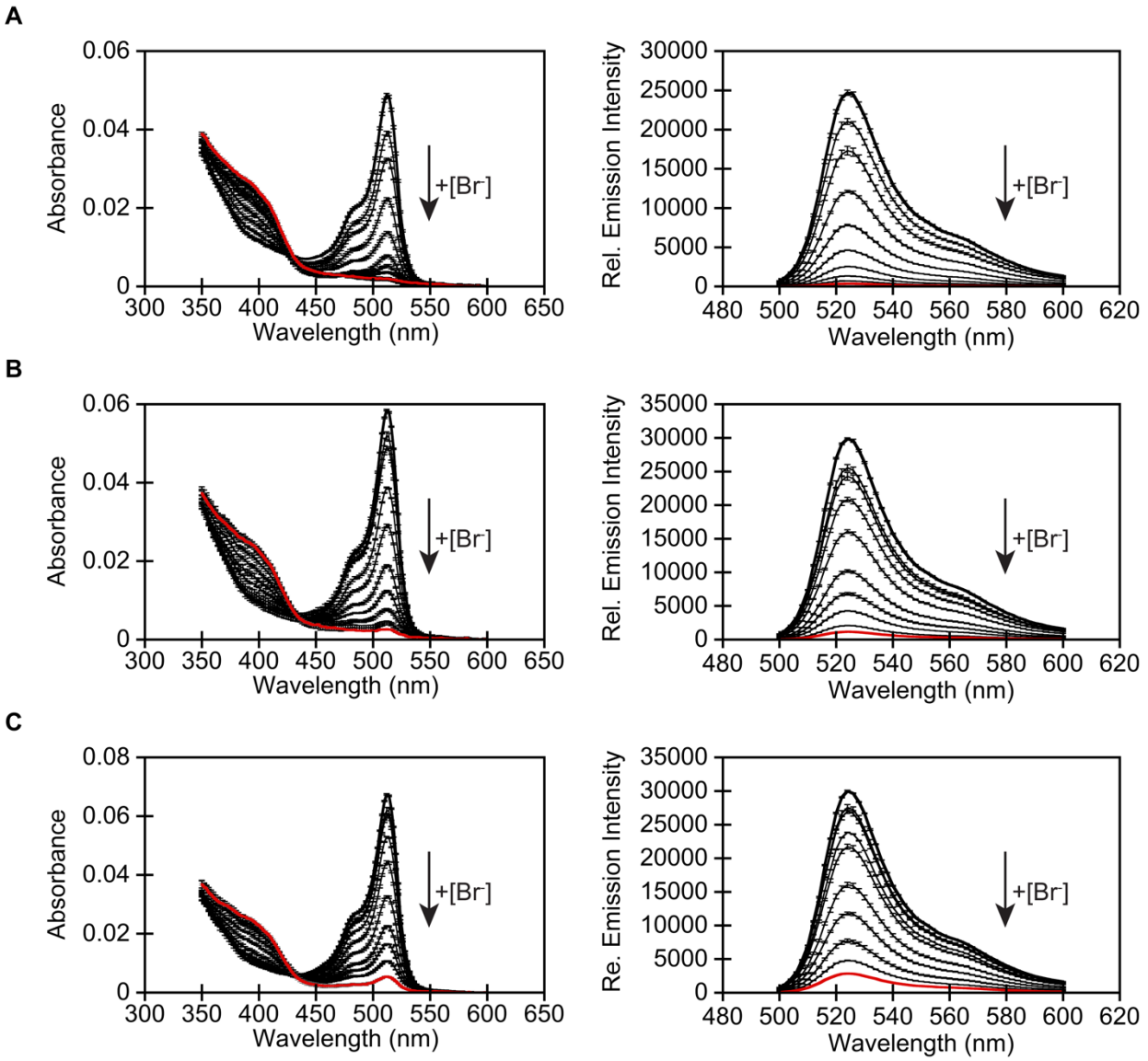

Figure S12. Absorbance (left) and emission spectra (right) of GFPxm163 at (A) pH 6, (B) pH 6.5, and (C) pH 7 in the presence of 0 (bold black), 2, 4, 8, 16, 32, 64, 128, 256, and 512 (red) mM Br^-. Data is shown one of two protein preparations each measured in triplicate and reported as an average with the S.E.M. Data for the second protein preparation is shown in Figure S13. All experiments were carried out at room temperature (24–26 °C) with 1 μM of protein in the 50 mM sodium phosphate buffer for pH 6–7. Absorbance was collected from 350–600 nm. Excitation was provided at 480 nm, and emission was collected from 500–600 nm.

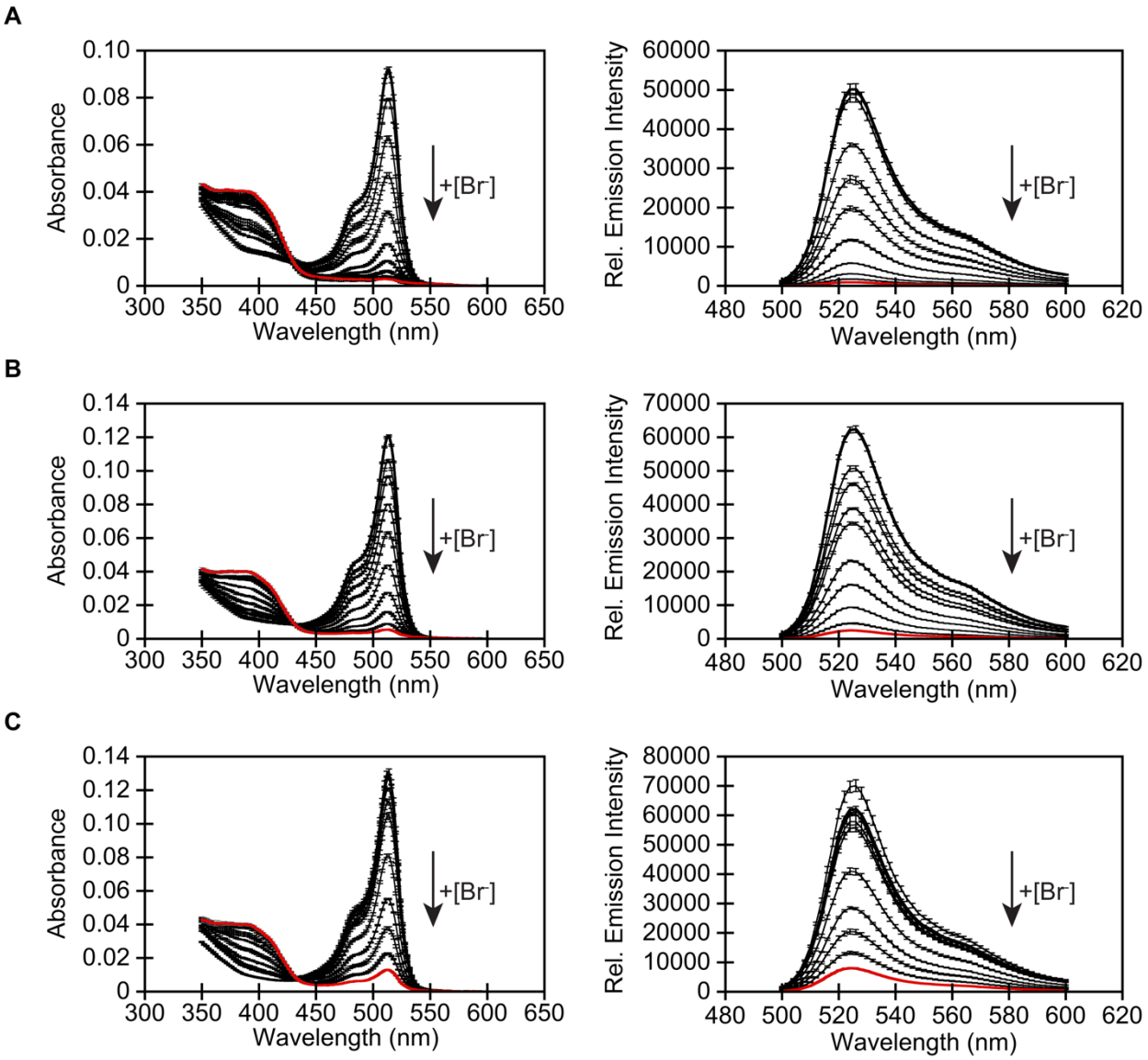

Figure S13. Absorbance (left) and emission spectra (right) of GFPxm163 at (A) pH 6, (B) pH 6.5, and (C) pH 7 in the presence of 0 (bold black), 2, 4, 8, 16, 32, 64, 128, 256, and 512 (red) mM Br^-. Data is shown one of two protein preparations each measured in triplicate and reported as an average with the S.E.M. Data for the first protein preparation is shown in Figure S12. All experiments were carried out at room temperature (24–26 °C) with 1.7 μM of protein in the 50 mM sodium phosphate buffer for pH 6–7. Absorbance was collected from 350–600 nm. Excitation was provided at 480 nm, and emission was collected from 500–600 nm.

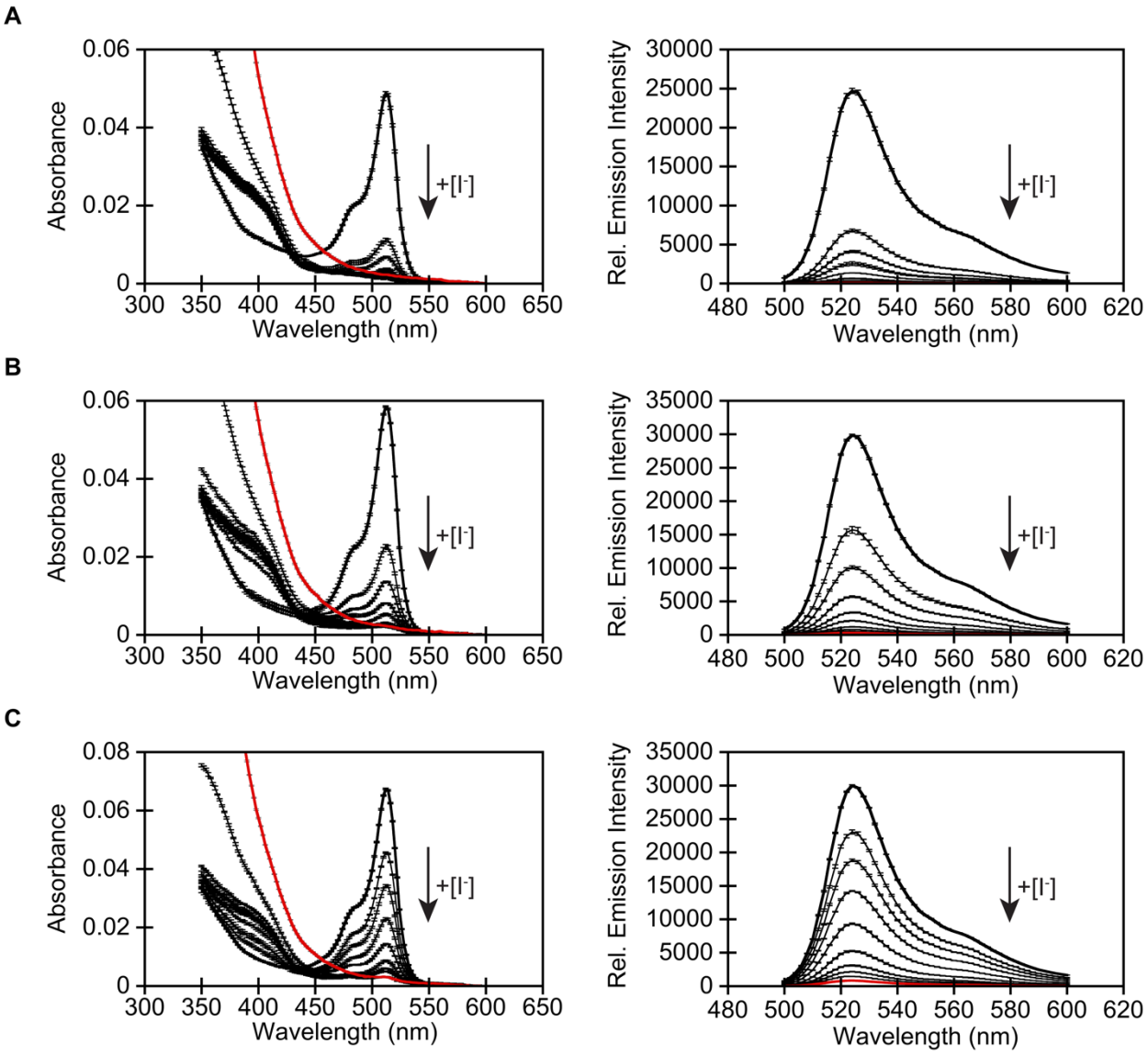

Figure S14. Absorbance (left) and emission spectra (right) of GFPxm163 at (A) pH 6, (B) pH 6.5, and (C) pH 7 in the presence of 0 (bold black), 2, 4, 8, 16, 32, 64, 128, 256, and 512 (red) mM I^-. Data is shown for one of two protein preparations each measured in triplicate and reported as an average with the S.E.M. Data for the second protein preparation is shown in Figure S15. All experiments were carried out at room temperature (24–26 °C) with 1 μM of protein in the 50 mM sodium phosphate buffer for pH 6–7. Absorbance was collected from 350–600 nm. Excitation was provided at 480 nm, and emission was collected from 500–600 nm.

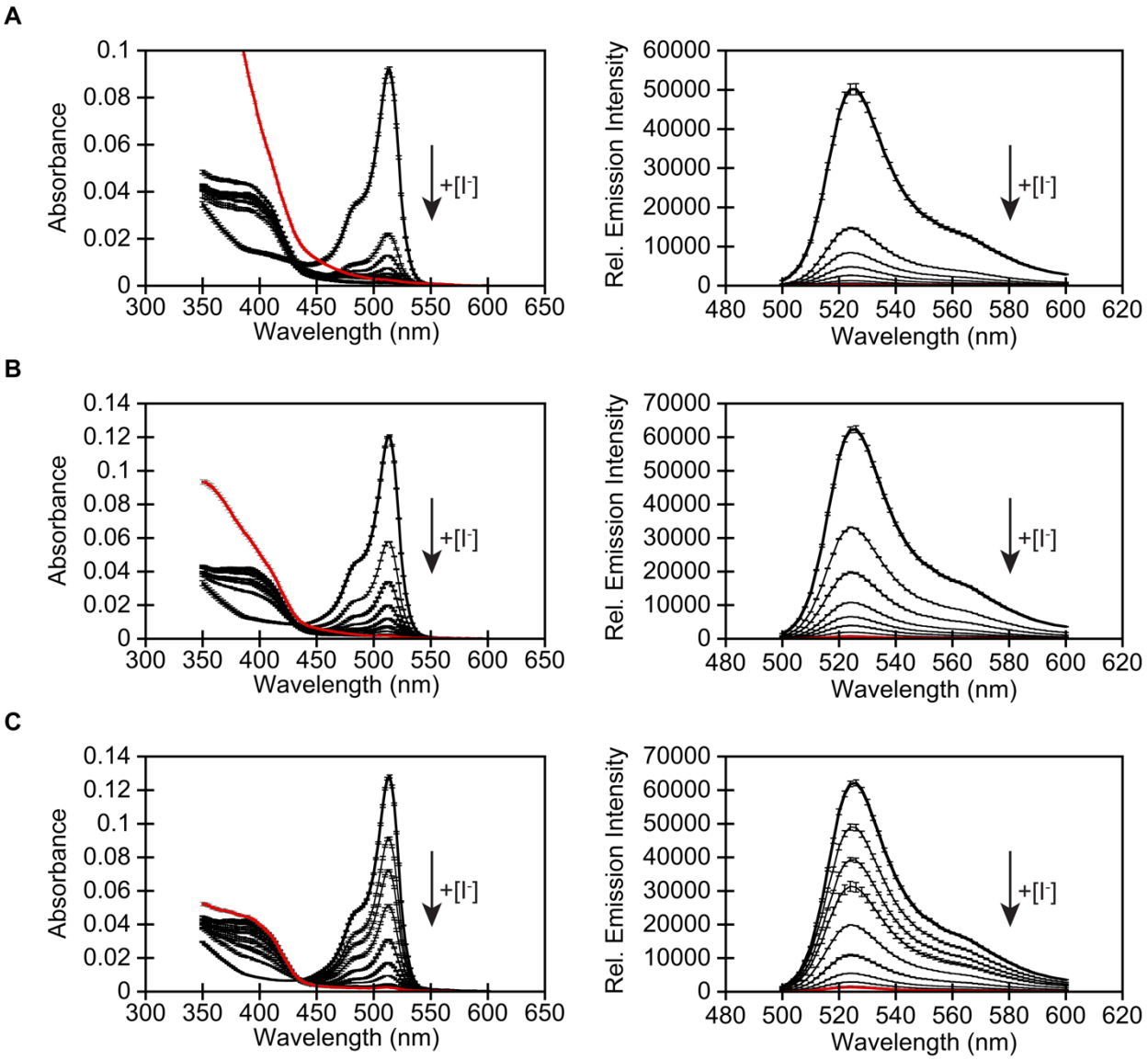

Figure S15. Absorbance (left) and emission spectra (right) of GFPxm163 at (A) pH 6, (B) pH 6.5, and (C) pH 7 in the presence of 0 (bold black), 2, 4, 8, 16, 32, 64, 128, 256, and 512 (red) mM I^-. Data is shown for one of two protein preparations each measured in triplicate and reported as an average with the S.E.M. Data for the first protein preparation is shown in Figure S14. All experiments were carried out at room temperature (24–26 °C) with 1.7 μM of protein in the 50 mM sodium phosphate buffer for pH 6–7. Absorbance was collected from 350–600 nm. Excitation was provided at 480 nm, and emission was collected from 500–600 nm.

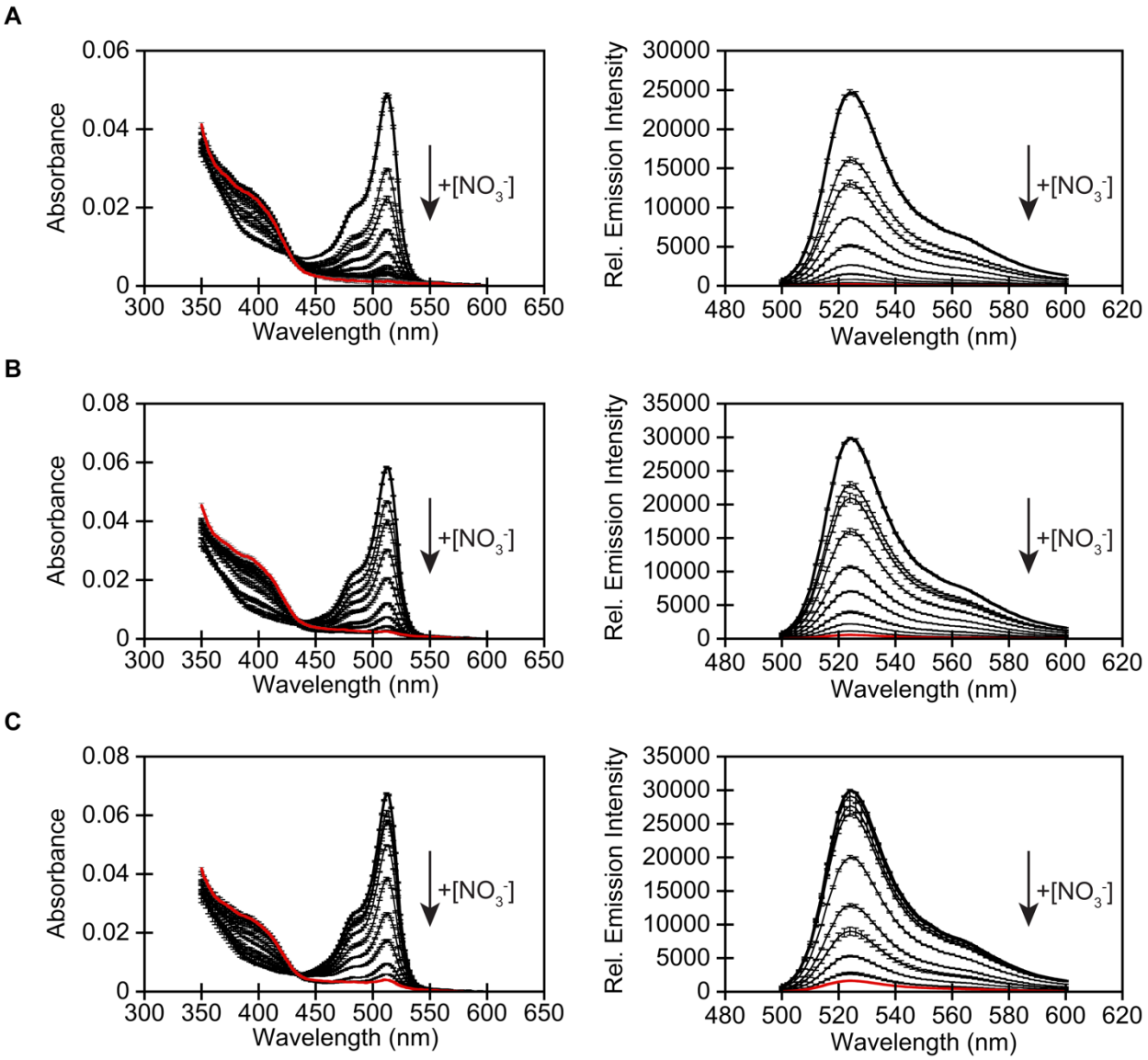

Figure S16. Absorbance (left) and emission spectra (right) of GFPxm163 at (A) pH 6, (B) pH 6.5, and (C) pH 7 in the presence of 0 (bold black), 2, 4, 8, 16, 32, 64, 128, 256, and 512 (red) mM NO_3^-. Data is shown for one of two protein preparations each measured in triplicate and reported as an average with the S.E.M. Data for the second protein preparation is shown in Figure S17. All experiments were carried out at room temperature (24–26 °C) with 1 μM of protein in the 50 mM sodium phosphate buffer for pH 6–7. Absorbance was collected from 350–600 nm. Excitation was provided at 480 nm, and emission was collected from 500–600 nm.

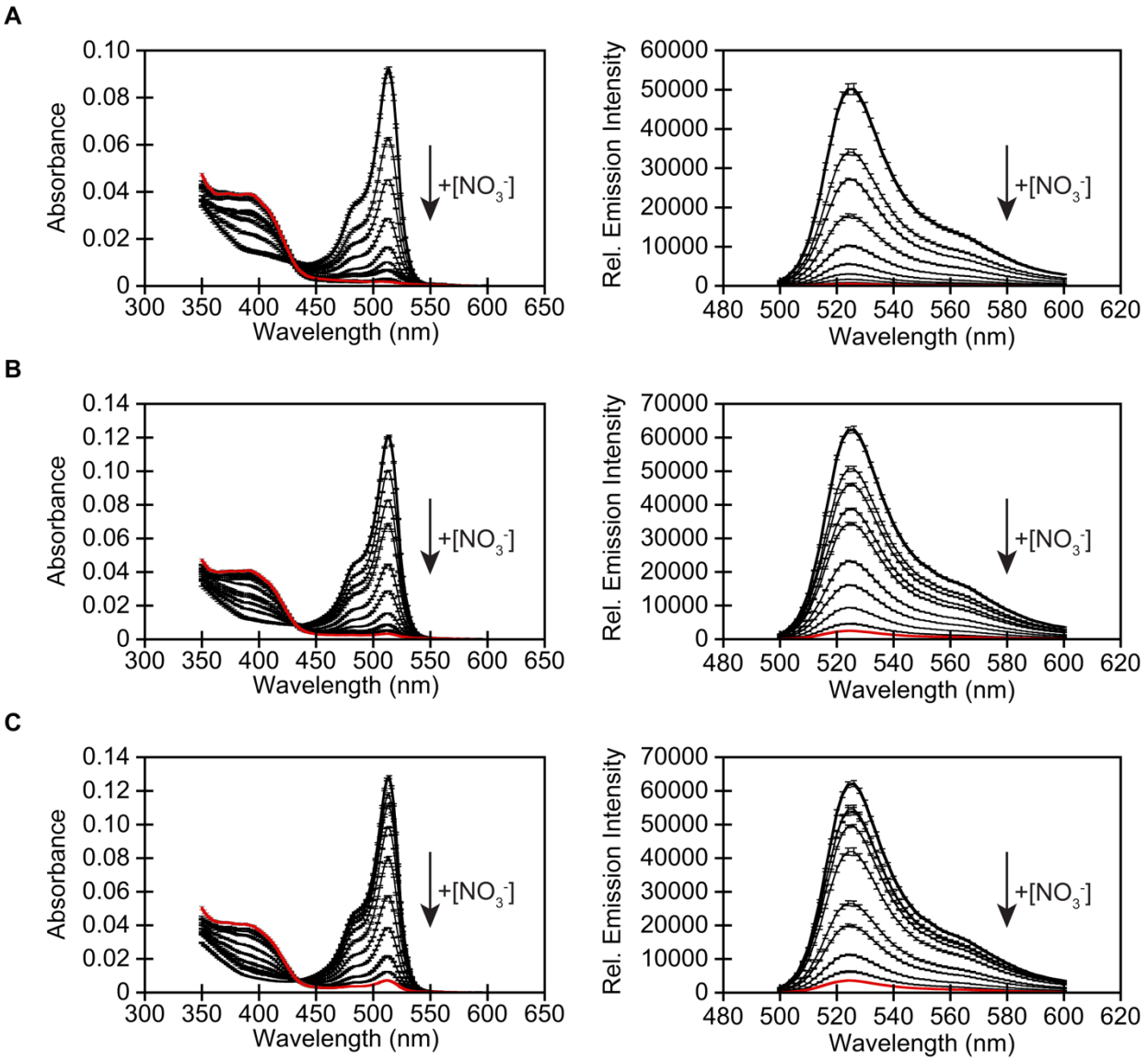

Figure S17. Absorbance (left) and emission spectra (right) of GFPxm163 at (A) pH 6, (B) pH 6.5, and (C) pH 7 in the presence of 0 (bold black), 2, 4, 8, 16, 32, 64, 128, 256, and 512 (red) mM NO_3^-. Data is shown for one of two protein preparations each measured in triplicate and reported as an average with the S.E.M. Data for the first protein preparation is shown in Figure S16. All experiments were carried out at room temperature (24–26 °C) with 1.7 μM of protein in the 50 mM sodium phosphate buffer for pH 6–7. Absorbance was collected from 350–600 nm. Excitation was provided at 480 nm, and emission was collected from 500–600 nm.

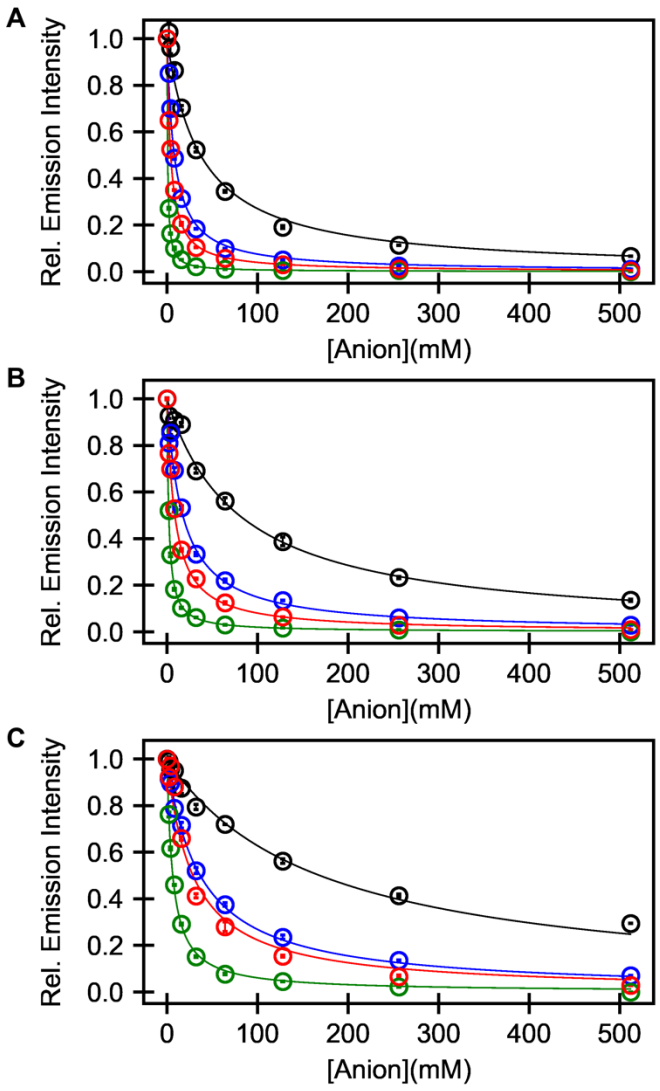

Figure S18. The average emission response of 1 μM GFPxm163 to Cl^- (black), Br^- (blue), I^- (green), and NO_3^- (red) from the anion titrations in Figure S8, S12, S14, and S16, respectively. The data was normalized to the emission response with the highest concentration of I^- tested. This normalized data was fitted to a single binding site model at (A) pH 6, (B) pH 6.5, and (C) pH 7 to calculate the apparent dissociation constants (K_d) reported in Table 1. Data is shown for one of two protein preparations each measured in triplicate and reported as an average with the S.E.M. Data for the second protein preparation is shown in Figure S19.

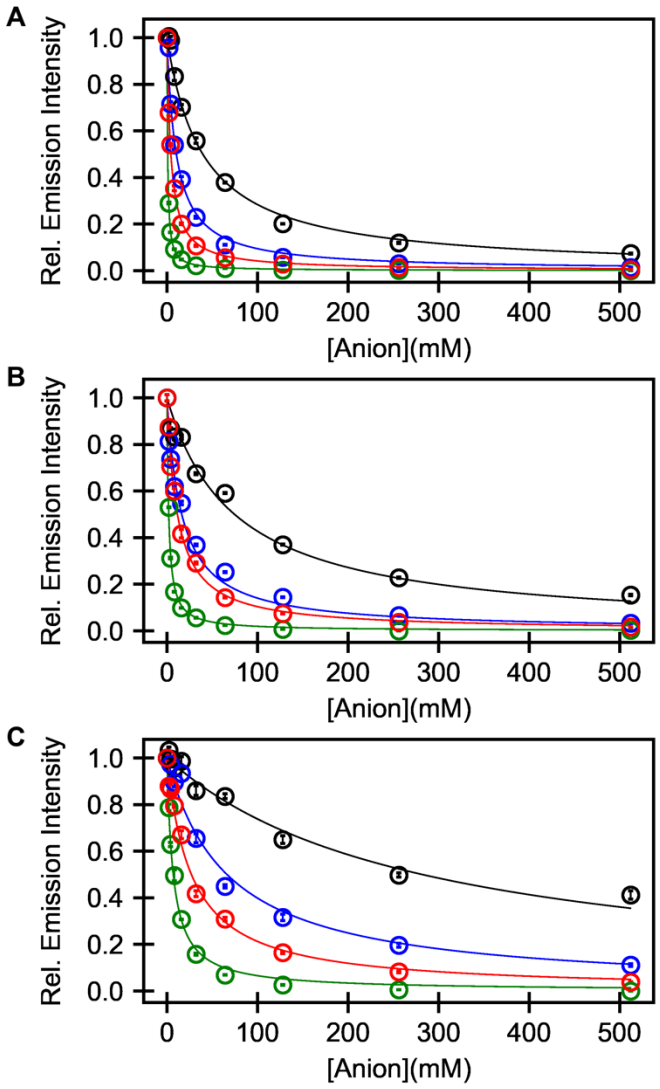

Figure S19. The average emission response of 1.7 µM GFPxm163 to Cl^- (black), Br^- (blue), I^- (green), and NO_3^- (red) from the anion titrations in Figure S9, S13, S15, and S17, respectively. The data was normalized to the emission response with the highest concentration of I^- tested. This normalized data was fitted to a single binding site model at (A) pH 6, (B) pH 6.5, and (C) pH 7 to calculate the apparent dissociation constants (K_d) reported in Table 1. Data is shown for one of two protein preparations each measured in triplicate and reported as an average with the S.E.M. Data for the first protein preparation is shown in Figure S18.

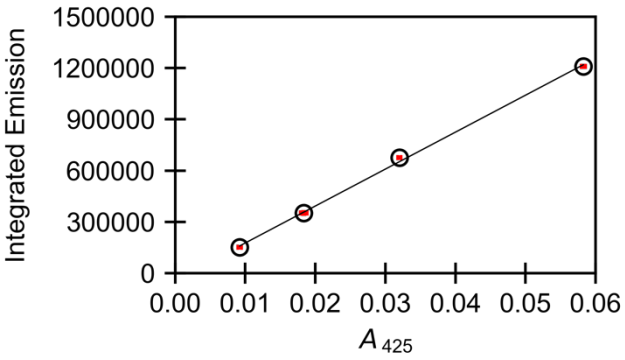

Figure S20. Fluorescence quantum yield standard curve for Coumarin 135 in 50% ethanol. The integrated emission is plotted versus the corrected absorbance intensity at 425 nm ($R^2 > 0.99$). Data at each concentration was collected in triplicate and is reported as an average with the S.E.M. All experiments were carried out at room temperature (24–26 °C). Excitation was provided at 425 nm, and emission was integrated from 440–800 nm.

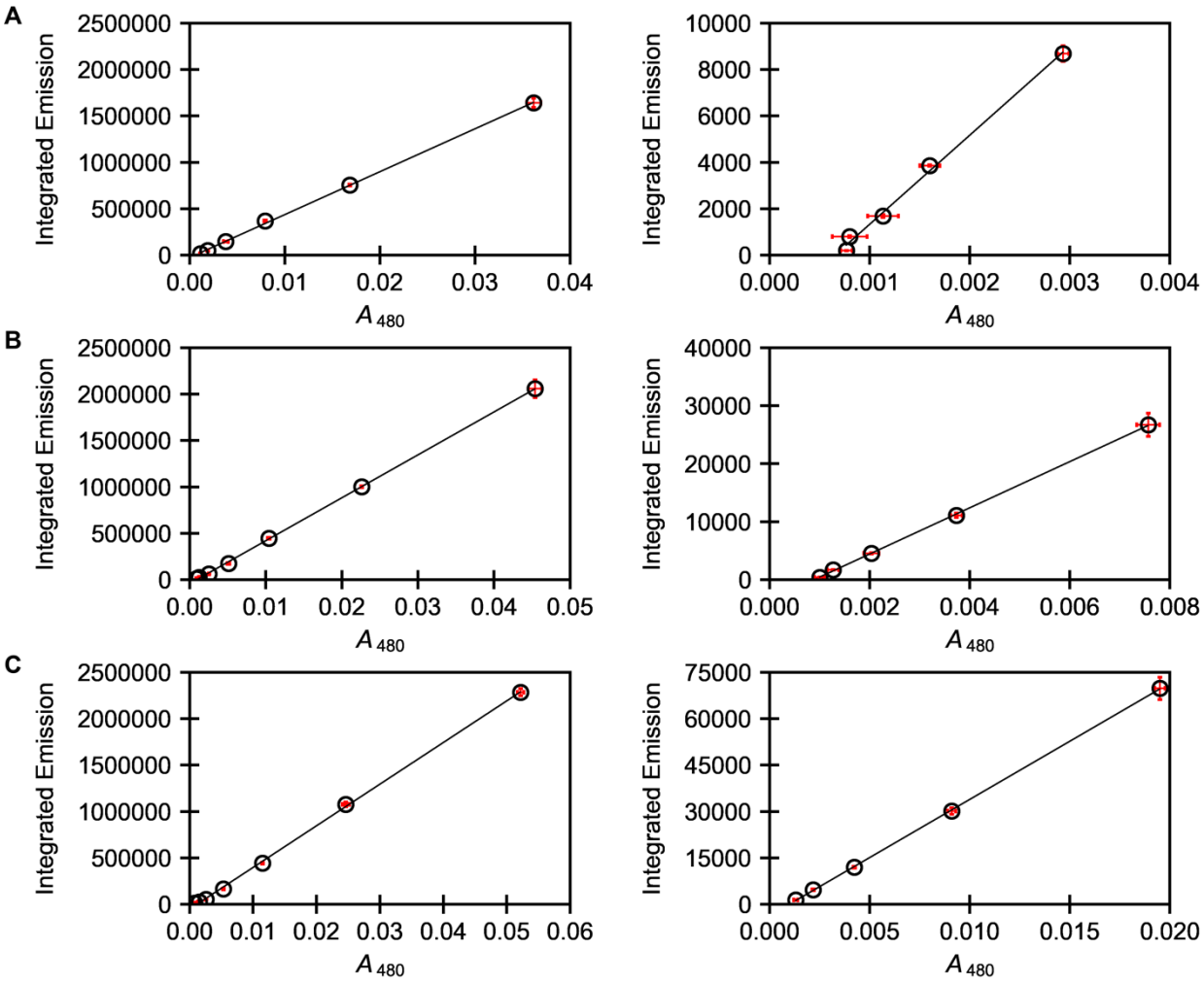

Figure S21. Fluorescence quantum yield curve for GFPxm163 at (A) pH 6, (B) pH 6.5, and (C) pH 7 in the absence (left) and presence (right) of 512 mM Cl^-. The integrated emission is plotted versus the corrected absorbance intensity at 480 nm ($R^2 > 0.99$). Data is shown for the first of three protein preparations each measured in triplicate and reported as an average with the S.E.M. Data for the second and third protein preparations are shown in Figures S22 and S23. All experiments were carried out at room temperature (24–26 °C) in 50 mM sodium phosphate buffer. Excitation was provided at 480 nm, and emission was integrated from 500–600 nm.

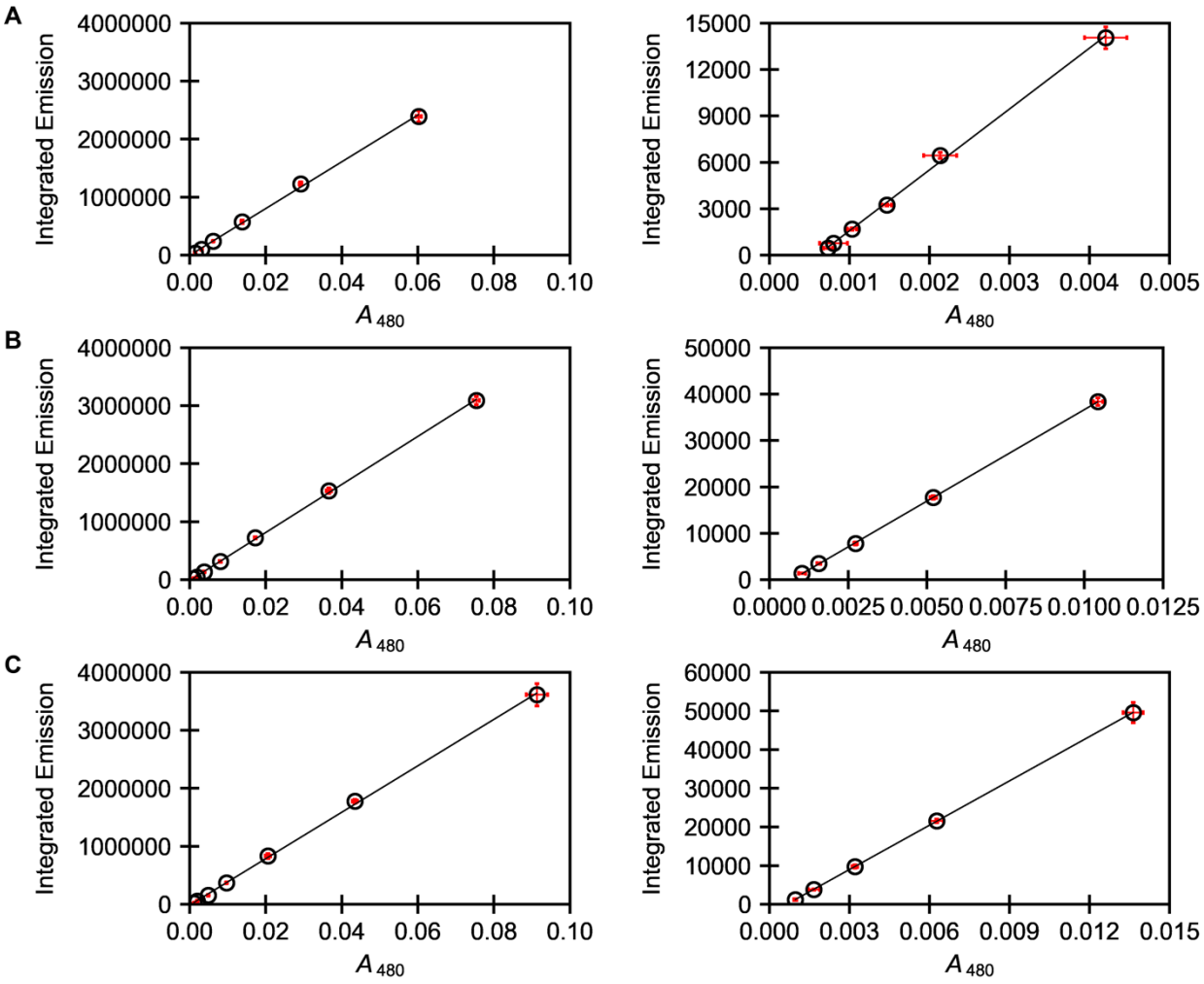

Figure S22. Fluorescence quantum yield curve for GFPxm163 at (A) pH 6, (B) pH 6.5, and (C) pH 7 in the absence (left) and presence (right) of 512 mM Cl^-. The integrated emission is plotted versus the corrected absorbance intensity at 480 nm ($R^2 > 0.99$). Data is shown for the second of three protein preparations each measured in triplicate and reported as an average with the S.E.M. Data for the first and third protein preparations are shown in Figures S21 and S23. All experiments were carried out at room temperature (24–26 °C) in 50 mM sodium phosphate buffer. Excitation was provided at 480 nm, and emission was integrated from 500–600 nm.

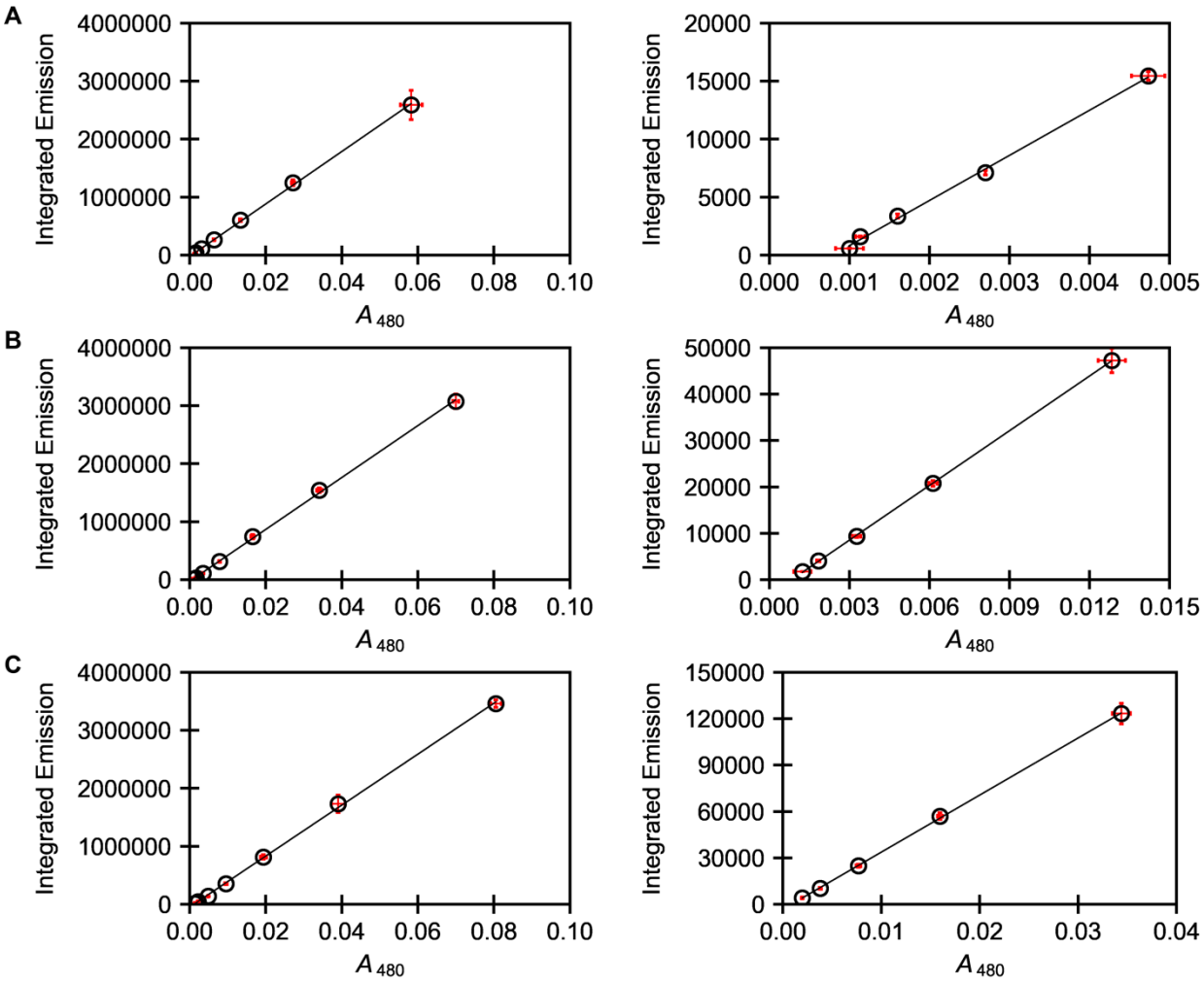

Figure S23. Fluorescence quantum yield curve for GFPxm163 at (A) pH 6, (B) pH 6.5, and (C) pH 7 in the absence (left) and presence (right) of 512 mM Cl^-. The integrated emission is plotted versus the corrected absorbance intensity at 480 nm ($R^2 > 0.99$). Data is shown for the third of three protein preparations each measured in triplicate and reported as an average with the S.E.M. Data for the first and second protein preparations are shown in Figures S21 and S22. All experiments were carried out at room temperature (24–26 °C) in 50 mM sodium phosphate buffer. Excitation was provided at 480 nm, and emission was integrated from 500–600 nm.

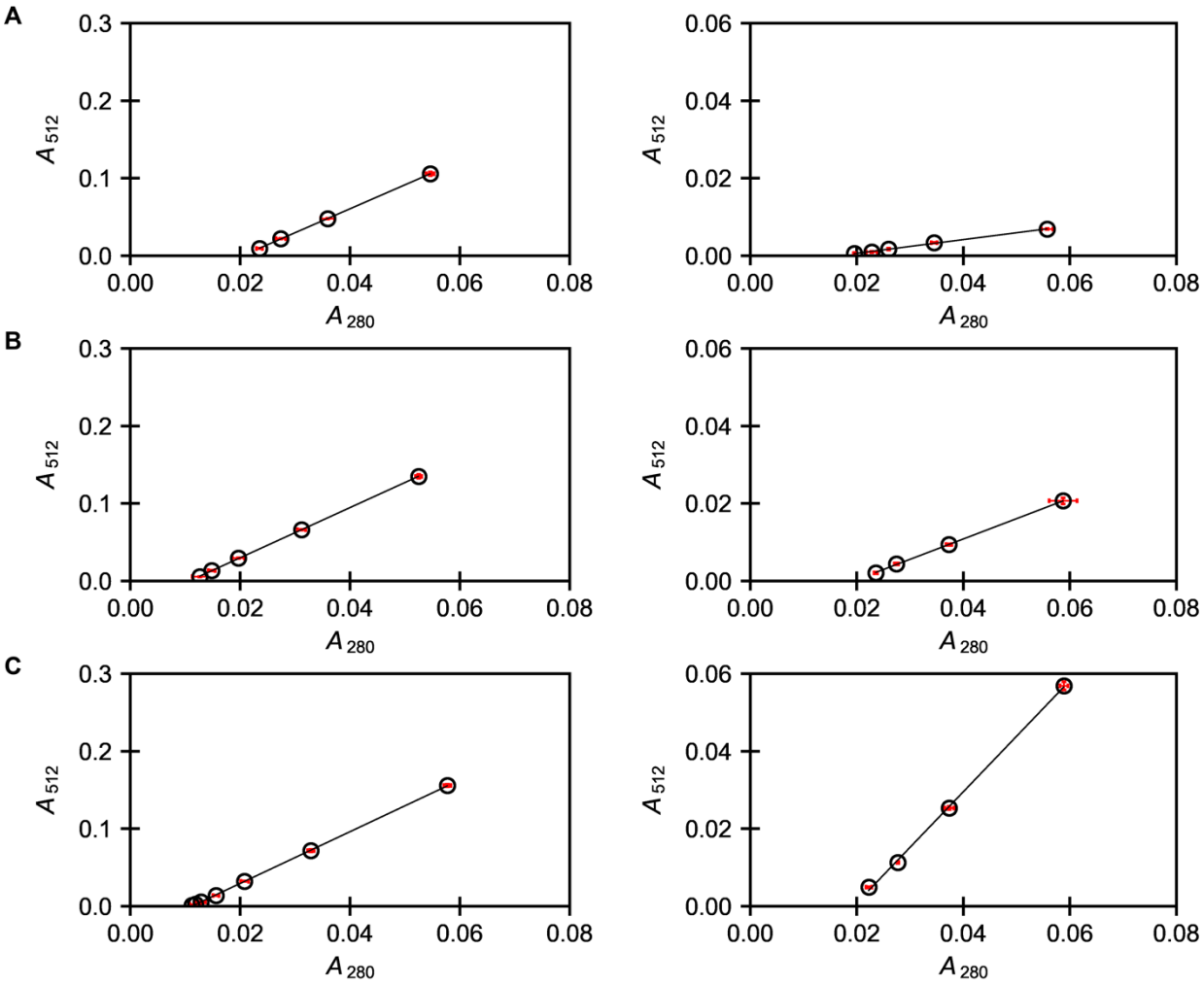

Figure S24. Extinction coefficient curve for GFPxm163 at (A) pH 6, (B) pH 6.5, and (C) pH 7 in the absence (left) and presence (right) of 512 mM Cl^-. The corrected absorbance intensity at 512 nm (A_{512}) is plotted versus the corrected absorbance intensity at 280 nm (A_{280}) ($R^2 > 0.99$). Data is shown for the first of three protein preparations each measured in triplicate and reported as an average with the S.E.M. Data for the second and third protein preparations are shown in Figures S25 and S26. All experiments were carried out at room temperature (24–26 °C) in 50 mM sodium phosphate buffer.

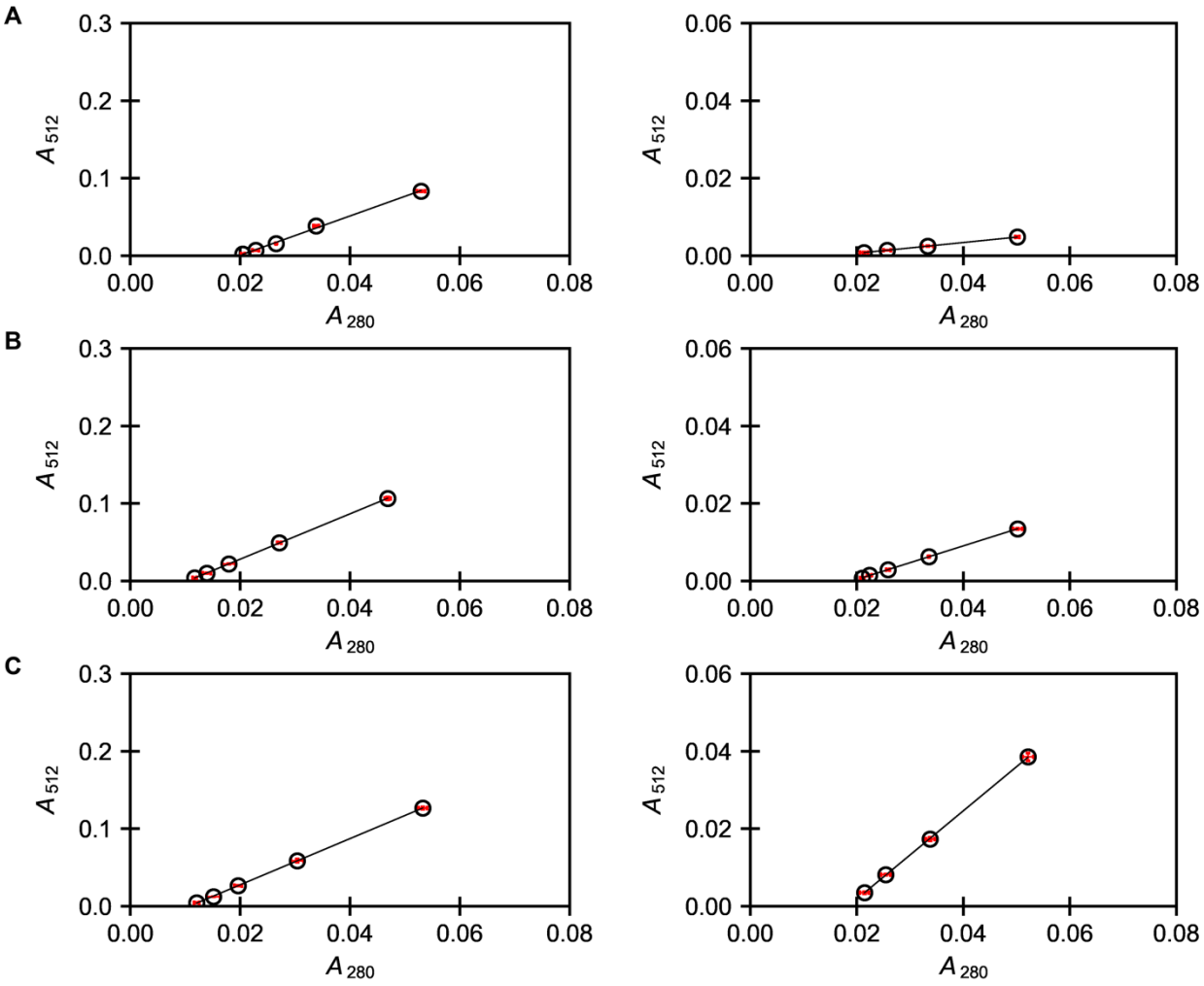

Figure S25. Extinction coefficient curve for GFPxm163 at (A) pH 6, (B) pH 6.5, and (C) pH 7 in the absence (left) and presence (right) of 512 mM Cl^-. The corrected absorbance intensity at 512 nm (A_{512}) is plotted versus the corrected absorbance intensity at 280 nm (A_{280}) ($R^2 > 0.99$). Data is shown for the second of three protein preparations each measured in triplicate and reported as an average with the S.E.M. Data for the first and third protein preparations are shown in Figures S24 and S26. All experiments were carried out at room temperature (24–26 °C) in 50 mM sodium phosphate buffer.

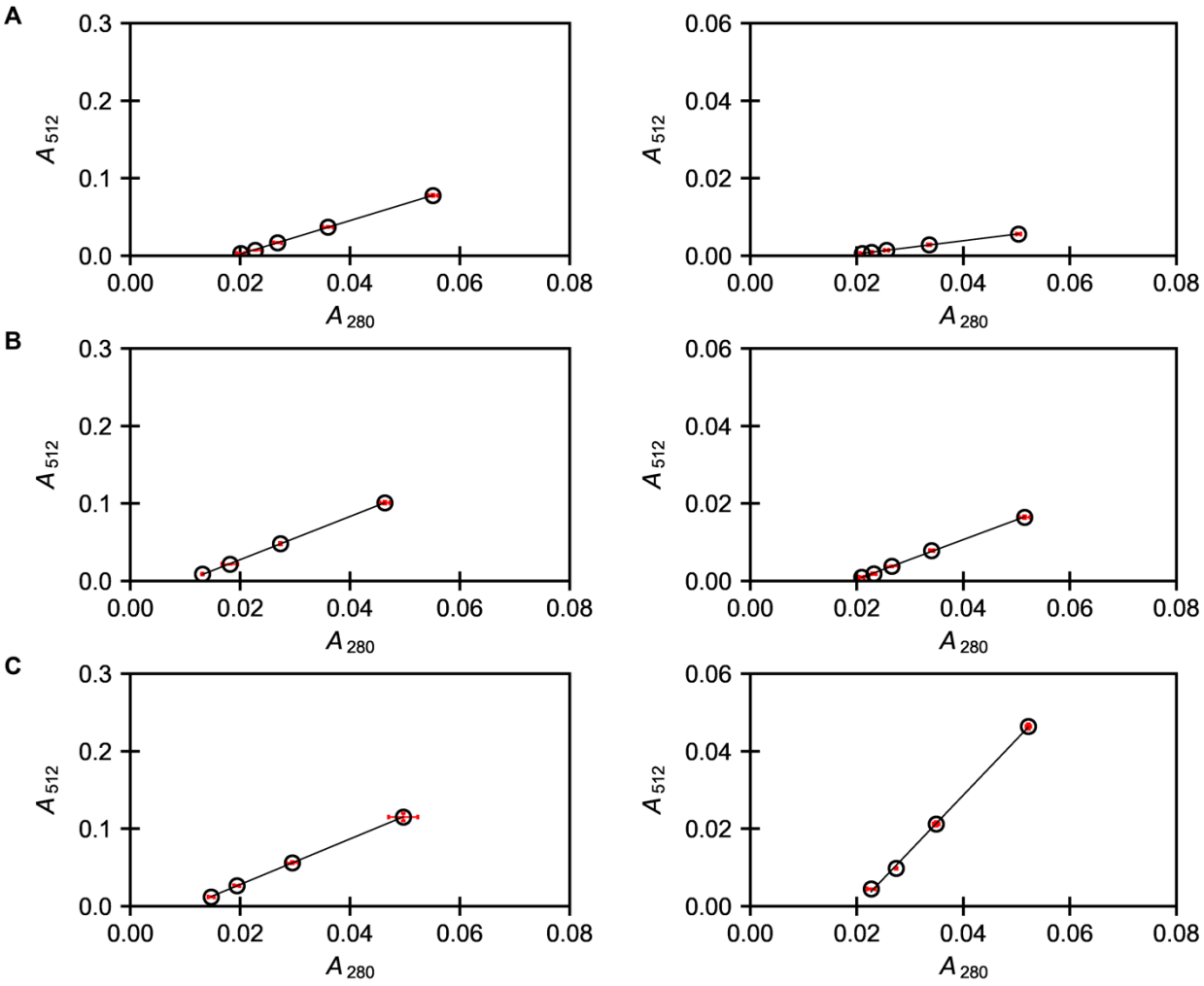

Figure S26. Extinction coefficient curve for GFPxm163 at (A) pH 6, (B) pH 6.5, and (C) pH 7 in the absence (left) and presence (right) of 512 mM Cl^-. The corrected absorbance intensity at 512 nm (A_{512}) is plotted versus the corrected absorbance intensity at 280 nm (A_{280}) ($R^2 > 0.99$). Data is shown for the third of three protein preparations each measured in triplicate and reported as an average with the S.E.M. Data for the first and second protein preparations are shown in Figures S24 and S25. All experiments were carried out at room temperature (24–26 °C) in 50 mM sodium phosphate buffer.

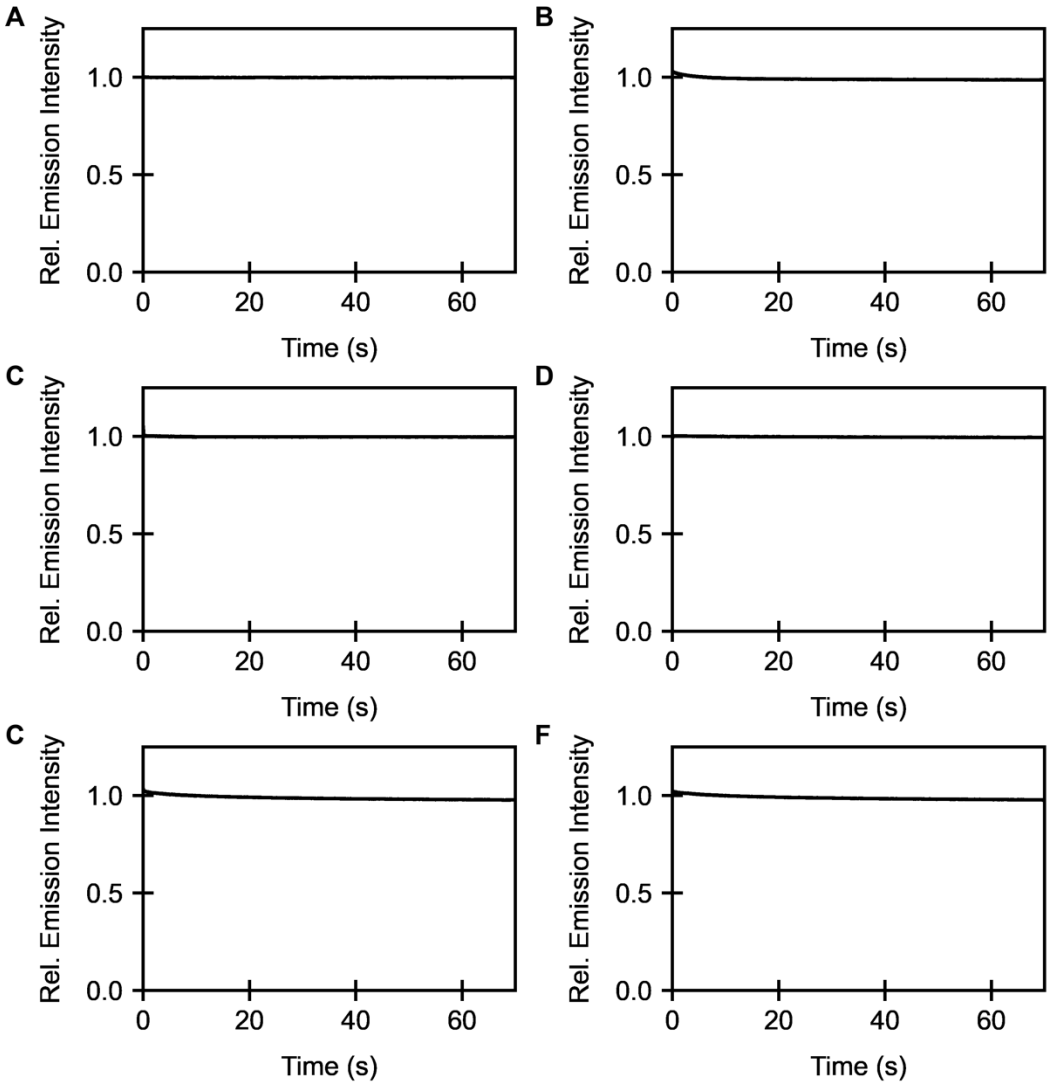

Figure S27. Stopped-flow fluorescence traces of GFPxm163 mixed with 50 mM sodium phosphate buffer at pH (A) 6, (B) 6.5, and (C) 7. In each row, data is shown for two different protein preparations across three technical replicates. Data from each protein preparation tested is reported as an average with the standard deviation (n = 15). All measurements were carried out at 22 °C. Excitation was provided at 500 nm with a 515 nm emission cutoff filter.

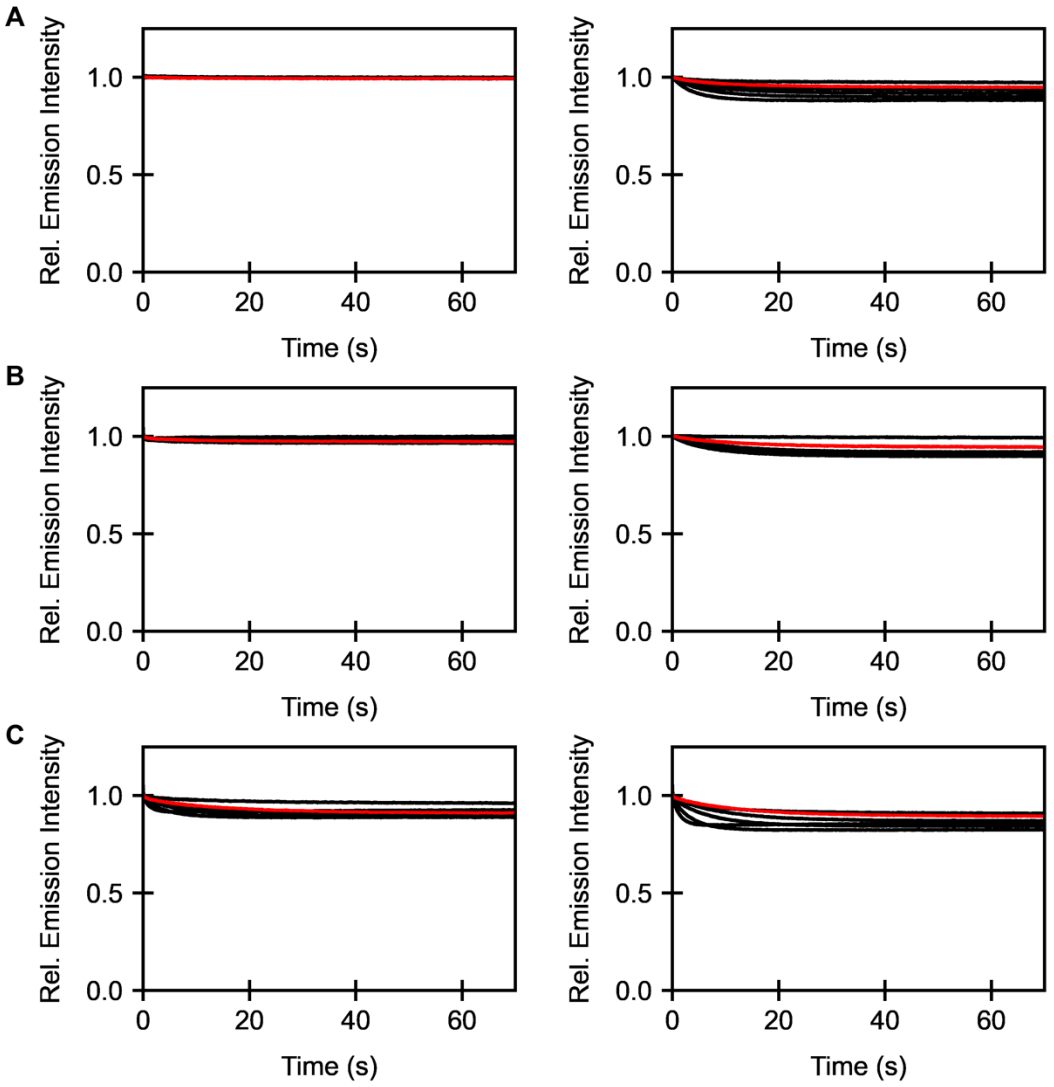

Figure S28. Stopped-flow fluorescence traces of GFPxm163 mixed with five different concentrations of Gluc in 50 mM sodium phosphate buffer at pH (A) 6, (B) 6.5, and (C) 7. The red line corresponds to the highest Gluc concentration. In each row, data is shown for two different protein preparations across three technical replicates. Data from each protein preparation is reported as an average with the standard deviation. All measurements were carried out at 22 °C. Excitation was provided at 500 nm with a 515 nm emission cutoff filter. The Gluc solutions were prepared at five linearly spaced concentrations from 32–96 mM and 64–192 mM for pH 6, 80–240 mM for pH 6.5, and 250–750 mM for pH 7.

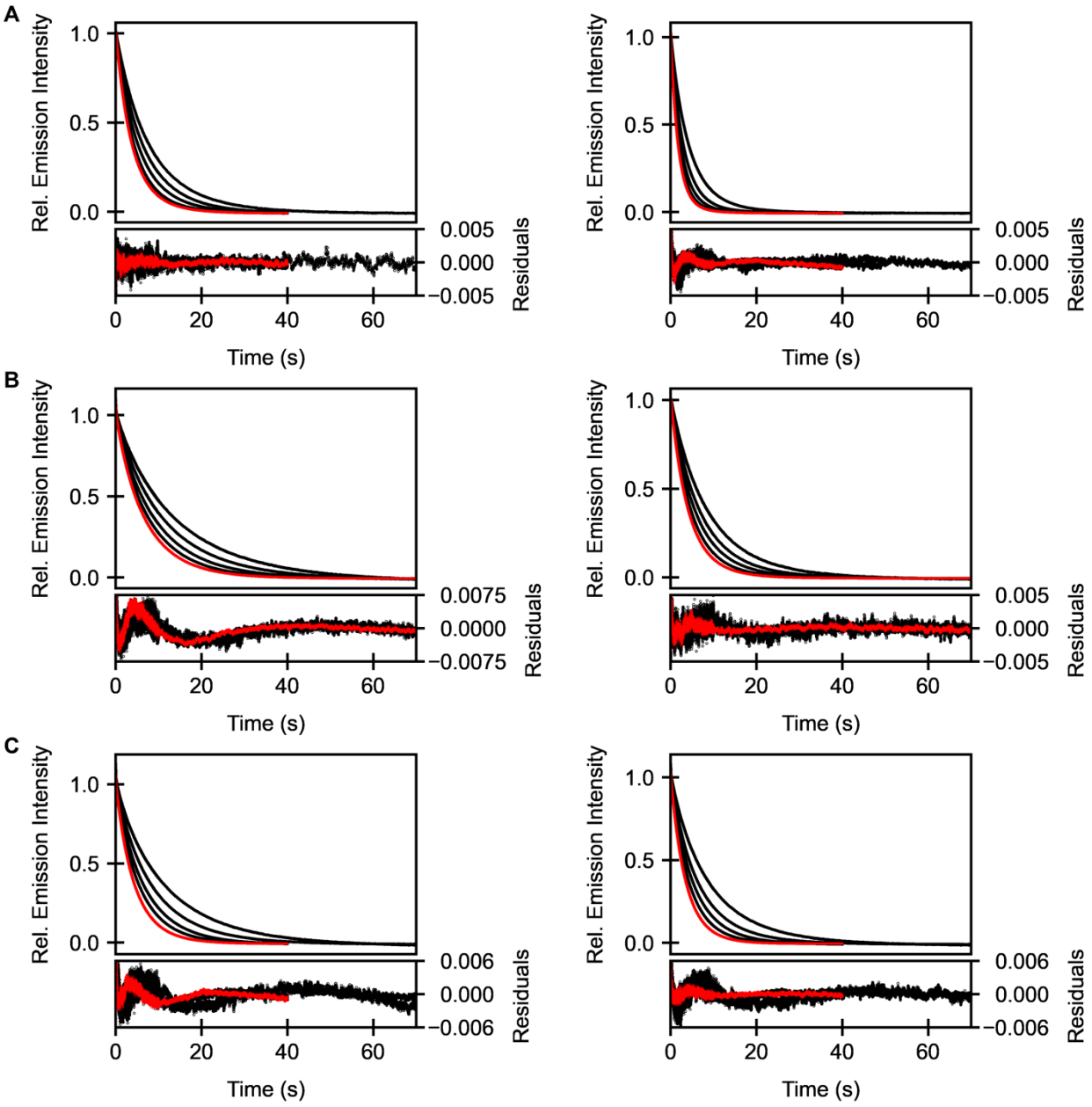

Figure S29. Stopped-flow fluorescence traces of GFPxm163 mixed with five different concentrations of Cl^- in 50 mM sodium phosphate buffer at pH (A) 6, (B) 6.5, and (C) 7 with plots of the residuals at each time point from fitting to a double exponential model. The red line corresponds to the highest Cl^- concentration. In each row, data is shown for two different protein preparations across three technical replicates. Data from each protein preparation is reported as an average with the standard deviation. All measurements were carried out at 22 °C. Excitation was provided at 500 nm with a 515 nm emission cutoff filter. The Cl^- solutions were prepared at five linearly spaced concentrations from 32–96 mM and 64–192 mM for pH 6, 80–240 mM for pH 6.5, and 250–750 mM for pH 7.

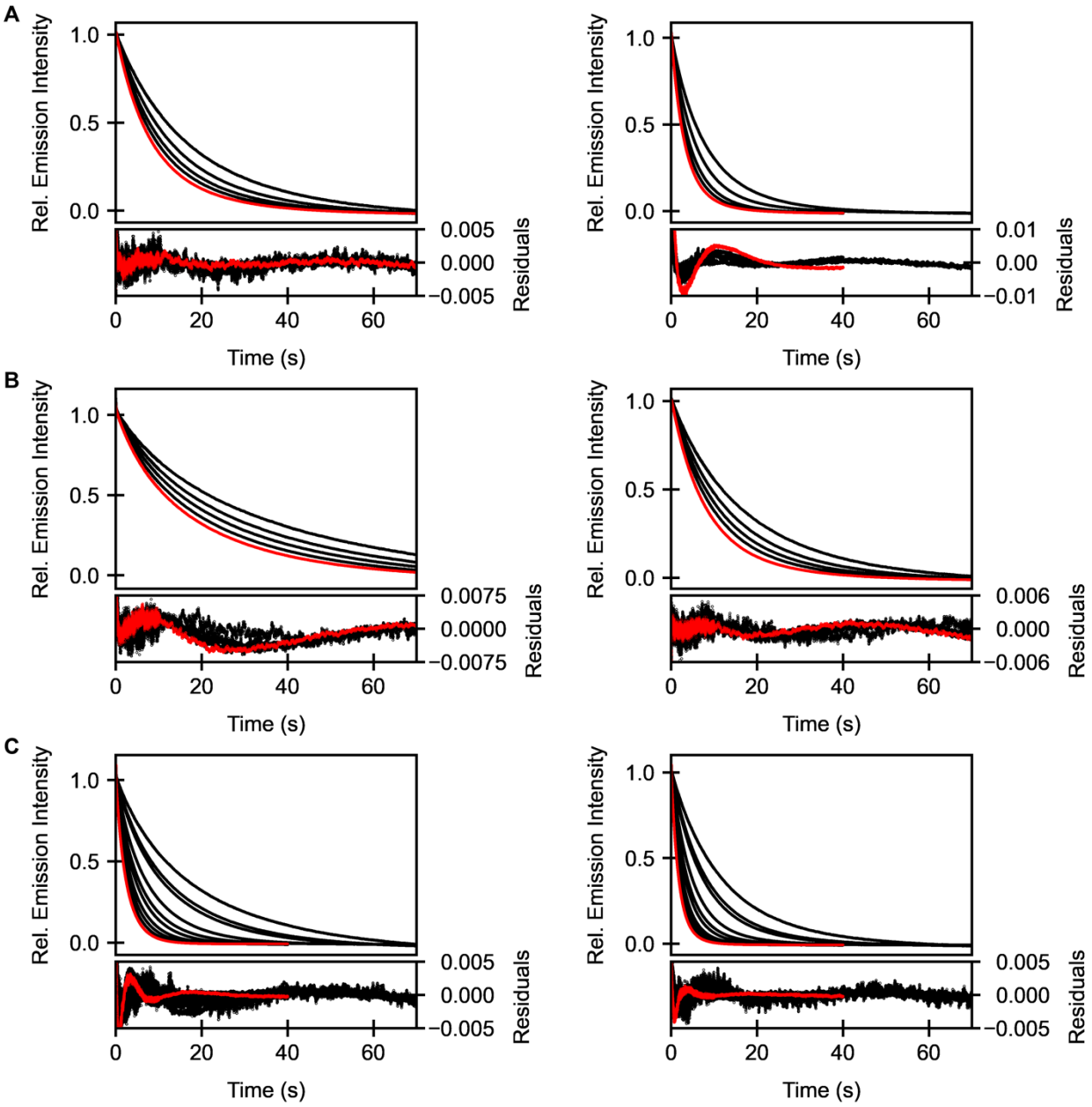

Figure S30. Stopped-flow fluorescence traces of GFPxm163 mixed with five different concentrations of Br^- in 50 mM sodium phosphate buffer at pH (A) 6, (B) 6.5, and (C) 7 with plots of the residuals at each time point from fitting to a double exponential model. The red line corresponds to the highest Br^- concentration. In each row, data is shown for two different protein preparations across three technical replicates. Data from each protein preparation is reported as an average with the standard deviation. All measurements were carried out at 22 °C. Excitation was provided at 500 nm with a 515 nm emission cutoff filter. The Br^- solutions were prepared at five linearly spaced concentrations from 8–24 mM and 16–48 mM for pH 6, 20–60 mM for pH 6.5, and ten concentrations from 75–750 mM for pH 7.

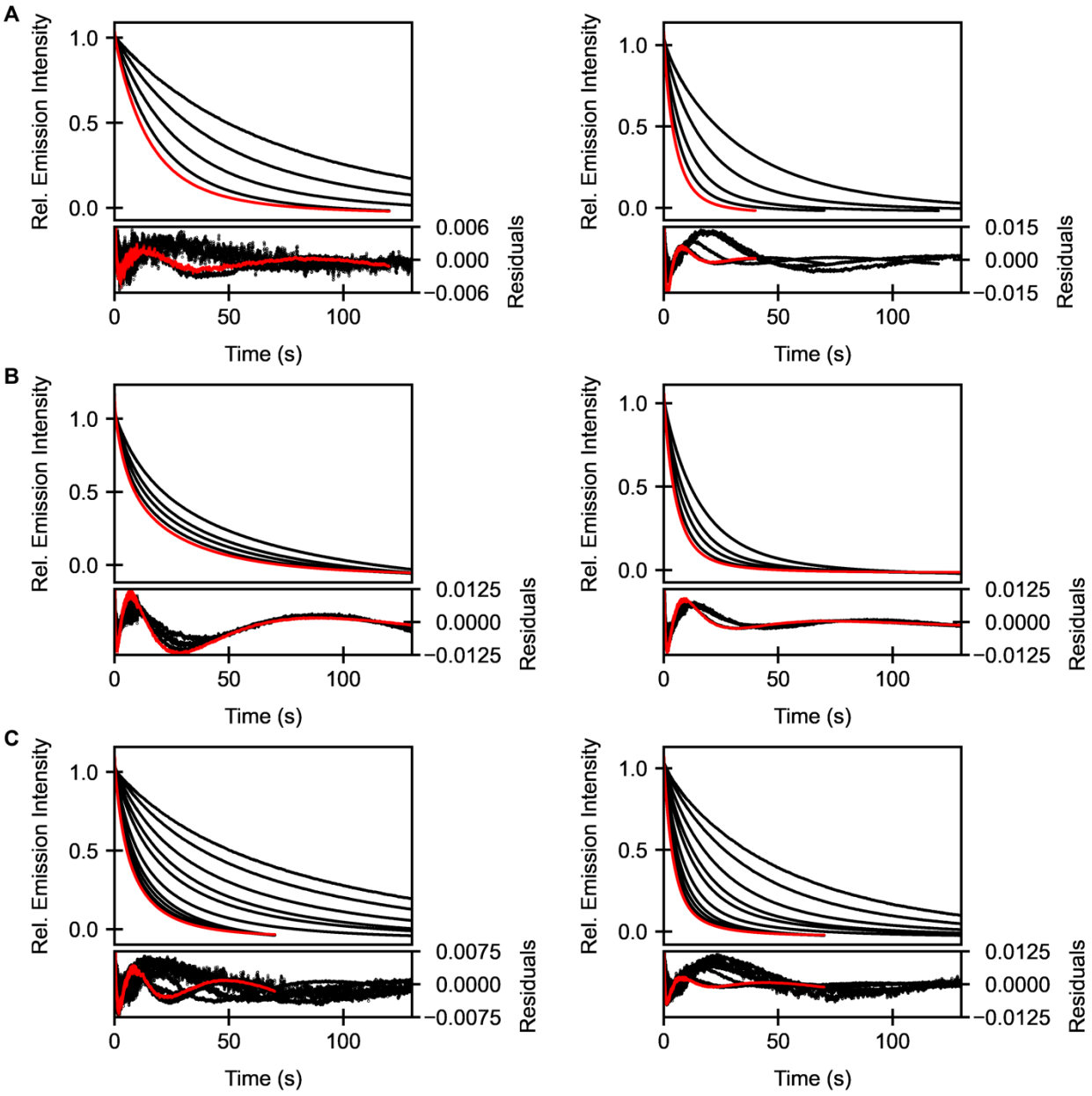

Figure S31. Stopped-flow fluorescence traces of GFPxm163 mixed with five different concentrations of I^- in 50 mM sodium phosphate buffer at pH (A) 6, (B) 6.5, and (C) 7 with plots of the residuals at each time point from fitting to a double exponential model. The red line corresponds to the highest I^- concentration. In each row, data is shown for two different protein preparations across three technical replicates. Data from each protein preparation is reported as an average with the standard deviation. All measurements were carried out at 22 °C. Excitation was provided at 500 nm with a 515 nm emission cutoff filter. The I^- solutions were prepared at concentrations of 1, 2, 4, 6, and 8 mM and 2, 4, 8, 12, and 16 mM for pH 6, five linearly spaced concentrations from 20–60 mM for pH 6.5, and ten concentrations from 8–160 mM for pH 7.

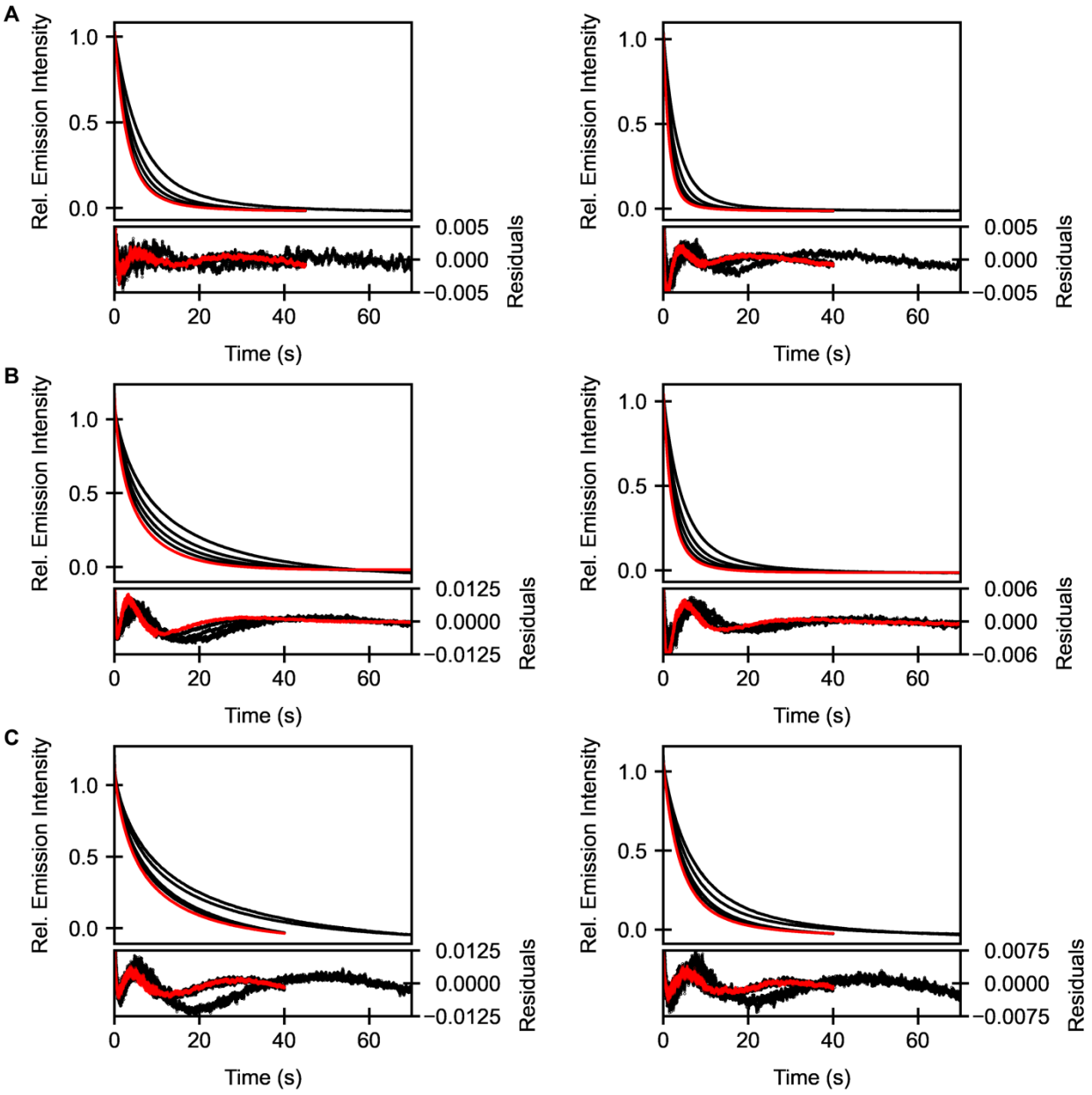

Figure S32. Stopped-flow fluorescence traces of GFPxm163 mixed with five different concentrations of NO_3^- in 50 mM sodium phosphate buffer at pH (A) 6, (B) 6.5, and (C) 7 with plots of the residuals at each time point from fitting to a double exponential model. The red line corresponds to the highest NO_3^- concentration. In each row, data is shown for two different protein preparations across three technical replicates. Data from each protein preparation is reported as an average with the standard deviation. All measurements were carried out at 22 °C. Excitation was provided at 500 nm with a 515 nm emission cutoff filter. The NO_3^- solutions were prepared at five linearly spaced concentrations from 4–12 mM and 8–24 mM for pH 6, 20–60 mM for pH 6.5, and 24–72 mM for pH 7.

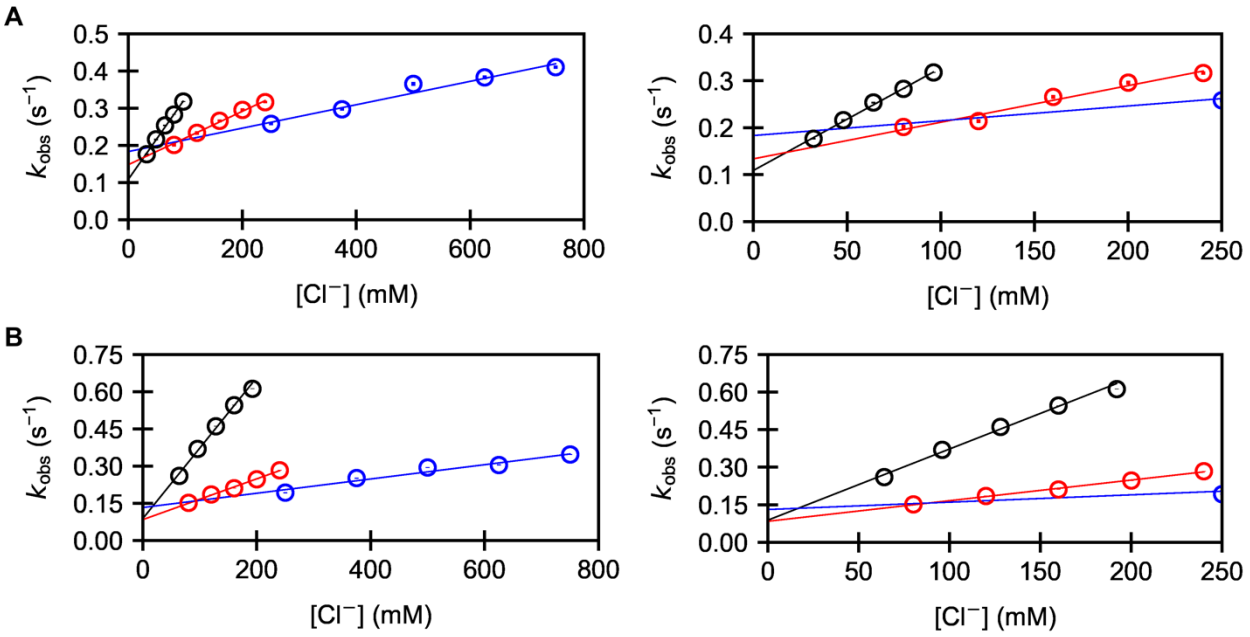

Figure S33. Relationship between the observed rate constant of binding (k_{obs}) for GFPxm163 as a function of Cl^- concentration (shown on the left with a zoomed view on the right) at pH 6 (black), 6.5 (red), and 7 (blue) determined from the stopped-flow fluorescence measurements in Figure S29. The weighted linear regression with the standard deviation of the k_{obs} at each anion concentration is shown for the (A) first and (B) second protein preparations.

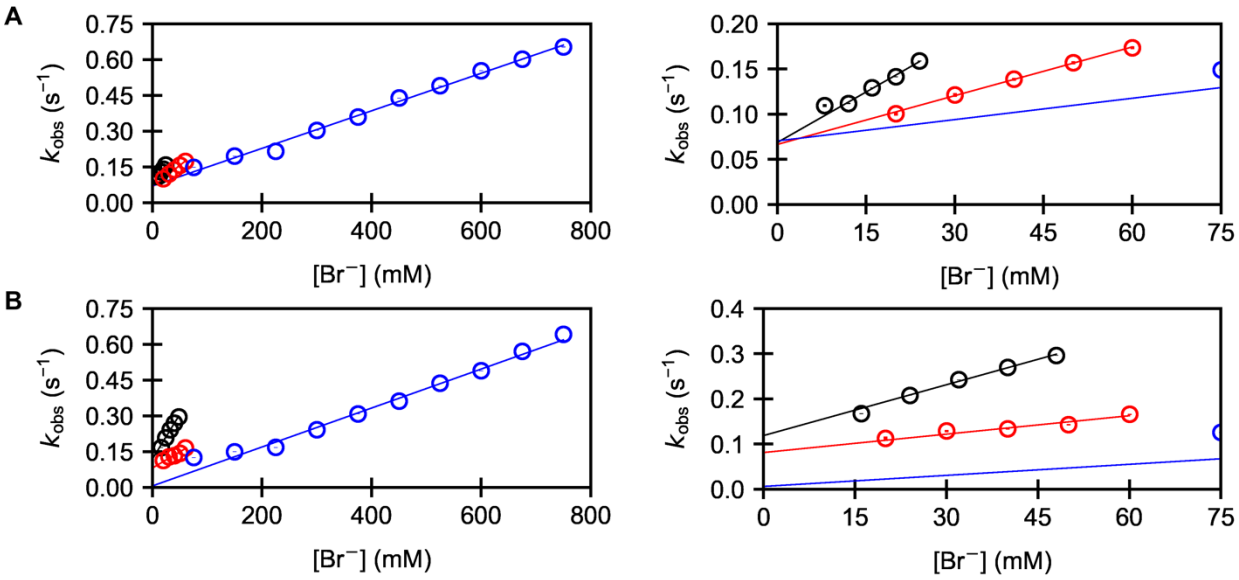

Figure S34. Relationship between the observed rate constant of binding (k_{obs}) for GFPxm163 as a function of Br^- concentration (shown on the left with a zoomed view on the right) at pH 6 (black), 6.5 (red), and 7 (blue) determined from the stopped-flow fluorescence measurements in Figure S30. The weighted linear regression with the standard deviation of the k_{obs} at each anion concentration is shown for the (A) first and (B) second protein preparations.

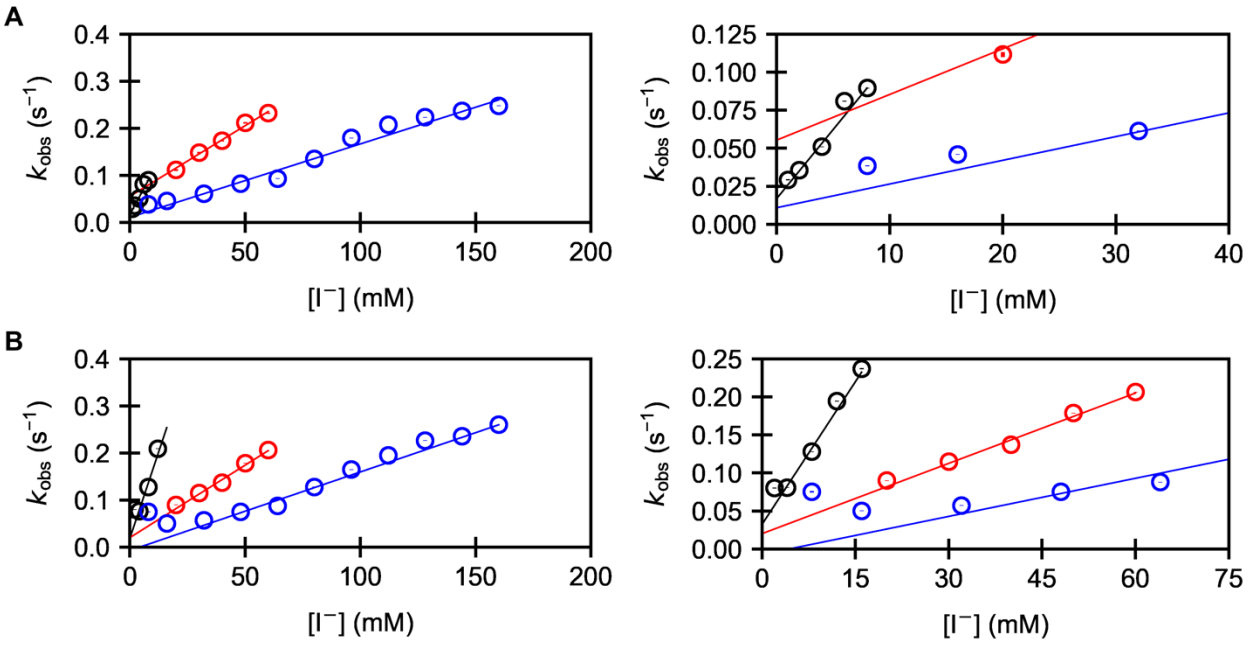

Figure S35. Relationship between the observed rate constant of binding (k_{obs}) for GFPxm163 as a function of I^- concentration (shown on the left with a zoomed view on the right) at pH 6 (black), 6.5 (red), and 7 (blue) determined from the stopped-flow fluorescence measurements in Figure S31. The weighted linear regression with the standard deviation of the k_{obs} at each anion concentration is shown for the (A) first and (B) second protein preparations.

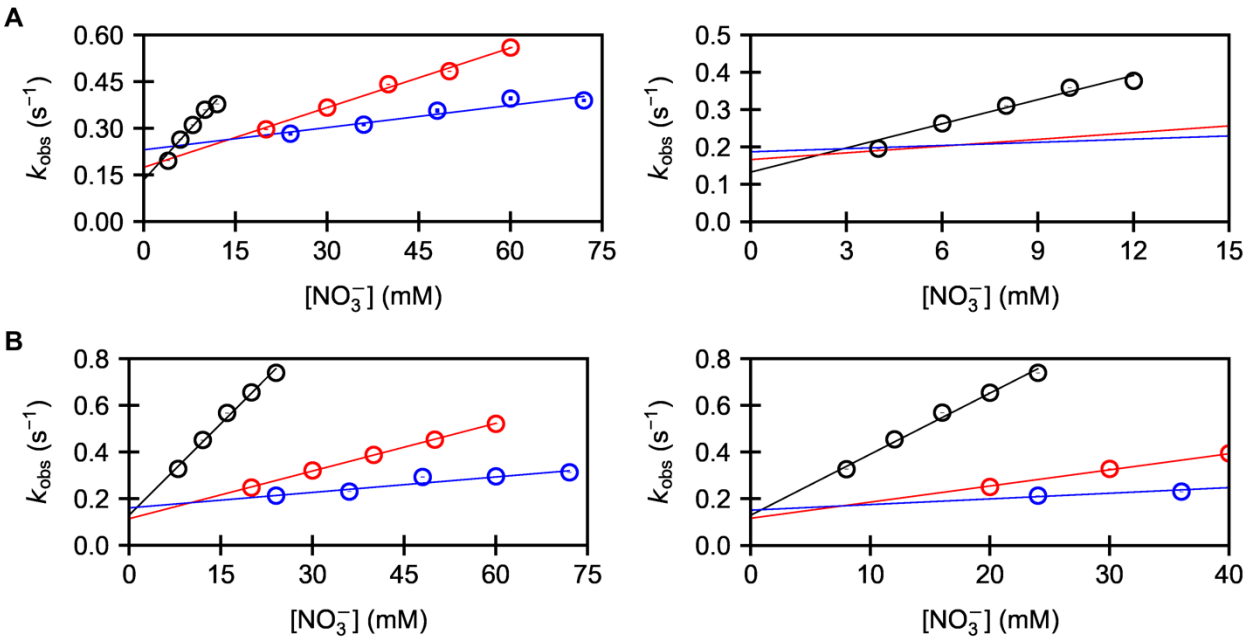

Figure S36. Relationship between the observed rate constant of binding (k_{obs}) for GFPxm163 as a function of NO_3^- concentration (shown on the left with a zoomed view on the right) at pH 6 (black), 6.5 (red), and 7 (blue) determined from the stopped-flow fluorescence measurements in Figure S32. The weighted linear regression with the standard deviation of the k_{obs} at each anion concentration is shown for the (A) first and (B) second protein preparations.

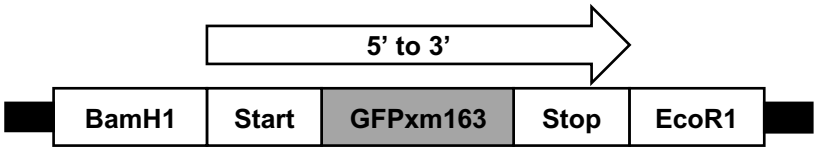

GGATCCATGTCTAAGGGGGAGGAGCTGTTTACTGGCATTGTGCCTGTGCTGATTGAGCTGGATGGGGATG
TGCATGGGCATAAGTTTTCCGTGAGAGGCGAGGGAGAGGGCGACGCAGATTATGGCAAGCTGGAGATCAA
GTTCATCTGCACCACAGGCAAGCTGCCCGTGCCTTGGCCAACCCTGGTGACCACACTGGGCTACGGCATC
CAGTGTTTTGCCAGGTATCCAGAGCACATGAAGATGAATGACTTCTTTAAGTCTGCCATGCCCGAGGGCT
ACATCCAGGAGAGGACAATCTTCTTTCAGGACGATGGCAAGTATAAGACCCGCGGCGAGGTGAAGTTCGA
GGGCGATACACTGGTGAACCGGATCGAGCTGAAGGGCATGGACTTCAAGGAGGATGGCAATATCCTGGGC
CACAAGCTGGAGTACAACTTTAATAGCCACAACGTGTATATCATGCCTGACAAGGCCAACAATGGCCTGA
AGGTGAACTTTAAGATCAGACACAATATTGAGGGCGGCGGCGTGCAGCTGGCAGACCACTATCAGACAAA
CGTGCCACTGGGCGATGGACCCGTGCTGATCCCTATCAATCACTACCTGAGCTATCAGACCGCCATCTCC
AAGGACCGGAACGAGACAAGAGATCACATGGTGTTTCTGGAGTTTTTCTCTGCTTGCGGGCACACCCACG
GAATGGACGAGCTGTATAAGTGAGAATTC

MSKGEELFTGIVPVLIELDGDVHGHKFSVRGEGEGDADYGKLEIKFICTTGKLPVPWPTLVTTLGYGIQC
FARYPEHMKMNDFFKSAMPEGYIQERTIFFQDDGKYKTRGEVKFEGDTLVNRIELKGMDFKEDGNILGHK
LEYNFNSHNVYIMPDKANNGLKVNFKIRHNIEGGGVQLADHYQTNVPLGDGPVLIPINHYLSYQTAISKD
RNETRDHMVFLEFFSACGHTHGMDELYK

Figure S37. Schematic of the GFPxm163-pcDNA3.1(+) plasmid design for protein expression in mammalian cells with the nucleotide (top) and amino acid (bottom) sequences used in this study.

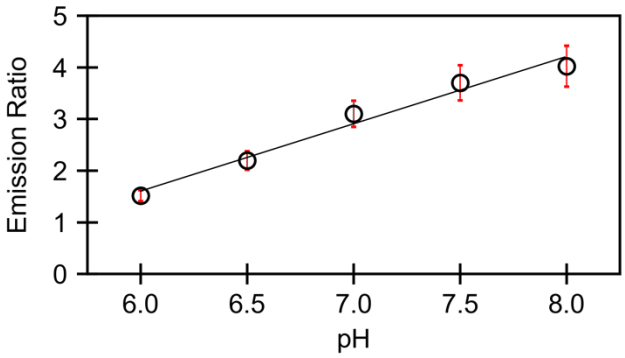

Figure S38. Linear calibration of pH versus the emission ratio (Ex_{490}/Ex_{440}) of live FRT-CFTR cells stained with 5 μM BCECF-AM dye at 37 °C in 10 mM HEPES buffer containing 137 mM KCl, 0.8 mM $CaCl_2$, 5 μM nigericin, and 5 μM valinomycin from pH 6–8. The averaged emission ratio of all regions of interest (n = 1,986) for six biological replicates with the S.E.M. is reported. The corresponding time-lapse fluorescence microscopy experiments are shown in ESI Movie 11–16.

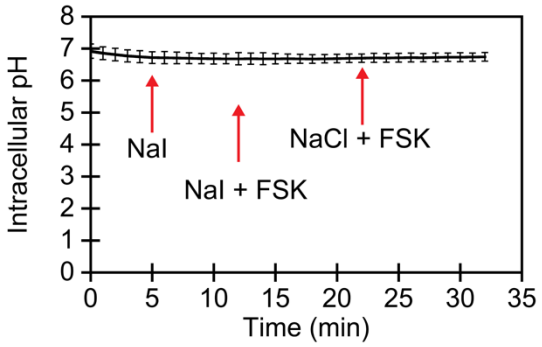

Figure S39. Plot of intracellular pH versus time for the Cl^-/I^- exchange in live FRT-CFTR cells stained with 5 μM BCECF-AM dye at 37 °C in a modified live cell imaging solution starting at pH 7.4 supplemented with 140 mM Cl^-, 40 mM Cl^-/100 mM I^-, 40 mM Cl^-/100 mM I^- with 20 μM FSK, and 140 mM Cl^- with 20 μM FSK. The averaged pH of all regions of interest (n = 2,185) for six biological replicates with the S.E.M. is reported. The corresponding time-lapse fluorescence microscopy experiments are shown in ESI Movie 17–22.

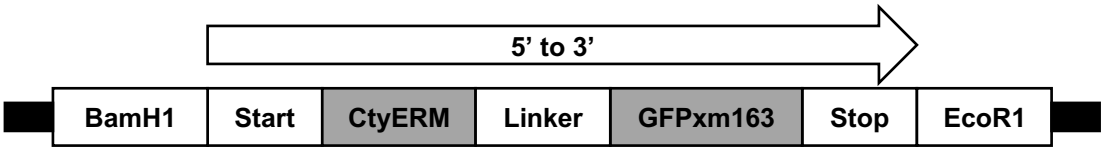

GGATCCGCCACCATGGACCCAGTGGTGGTGCTGGGCCTGTGCCTGTCTTGTCTGCTGCTGCTGAGCCTGT
GGAAGCAGTCCTACGGCGGCGGCAAGCTGAAGCTGAGAATCCTGCAGAGCACCGTGCCCCGGGCCAGAGA
TCCCCCTGTGGCCACATCTAAGGGGGAGGAGCTGTTTACTGGCATTGTGCCTGTGCTGATTGAGCTGGAT
GGGGATGTGCATGGGCATAAGTTTTCCGTGAGAGGCGAGGGAGAGGGCGACGCAGATTATGGCAAGCTGG
AGATCAAGTTCATCTGCACCACAGGCAAGCTGCCCGTGCCTTGGCCAACCCTGGTGACCACACTGGGCTA
CGGCATCCAGTGTTTTGCCAGGTATCCAGAGCACATGAAGATGAATGACTTCTTTAAGTCTGCCATGCCC
GAGGGCTACATCCAGGAGAGGACAATCTTCTTTCAGGACGATGGCAAGTATAAGACCCGCGGCGAGGTGA
AGTTCGAGGGCGATACACTGGTGAACCGGATCGAGCTGAAGGGCATGGACTTCAAGGAGGATGGCAATAT
CCTGGGCCACAAGCTGGAGTACAACTTTAATAGCCACAACGTGTATATCATGCCTGACAAGGCCAACAAT
GGCCTGAAGGTGAACTTTAAGATCAGACACAATATTGAGGGCGGCGGCGTGCAGCTGGCAGACCACTATC
AGACAAACGTGCCACTGGGCGATGGACCCGTGCTGATCCCTATCAATCACTACCTGAGCTATCAGACCGC
CATCTCCAAGGACCGGAACGAGACAAGAGATCACATGGTGTTTCTGGAGTTTTTCTCTGCTTGCGGGCAC
ACCCACGGAATGGACGAGCTGTATAAGTGAGAATTC

MDPVVVLGLCLSCLLLLSLWKQSYGGGKLKLRILQSTVPRARDPPVATSKGEELFTGIVPVLIELDGDVH
GHKFSVRGEGEGDADYGKLEIKFICTTGKLPVPWPTLVTTLGYGIQCFARYPEHMKMNDFFKSAMPEGYI
QERTIFFQDDGKYKTRGEVKFEGDTLVNRIELKGMDFKEDGNILGHKLEYNFNSHNVYIMPDKANNGLKV
NFKIRHNIEGGGVQLADHYQTNVPLGDGPVLIPINHYLSYQTAISKDRNETRDHMVFLEFFSACGHTHGM
DELYK

Figure S40. Schematic of the CytERM-GFPxm163-pcDNA3.1(+) plasmid design for protein expression in mammalian cells with the nucleotide (top) and amino acid (bottom) sequences used in this study.